Preclinical Evaluation of a Newcastle Disease Virus-Vectored Intranasal SARS-CoV-2 Vaccine

Manolo Fernandez Díaz
Farmacologicos Veterinarios S.A.C. FARVET
Katherine Calderón
Farmacologicos Veterinarios S.A.C. FARVET
Aldo Rojas-Neyra
Farmacologicos Veterinarios S.A.C. FARVET
Vikram N. Vakharia
University of Maryland Baltimore County
Ricardo Choque-Guevara
Farmacologicos Veterinarios S.A.C. FARVET
Angela Montalvan
Farmacologicos Veterinarios S.A.C. FARVET
Astrid Poma-Acevedo
Farmacologicos Veterinarios S.A.C. FARVET
Dora Rios-Matos
Farmacologicos Veterinarios S.A.C. FARVET
Andres Agurto- Arteaga
Farmacologicos Veterinarios S.A.C. FARVET
Maria de Grecia Cauti-Mendoza
Farmacologicos Veterinarios S.A.C. FARVET
Norma Perez-Martinez
Farmacologicos Veterinarios S.A.C. FARVET
Gisela Isasi-Rivas
Farmacologicos Veterinarios S.A.C. FARVET
Luis Tataje-Lavanda
Farmacologicos Veterinarios S.A.C. FARVET
Yacory Sernaque-Aguilar
Farmacologicos Veterinarios S.A.C. FARVET
Freddy Ygnacio-Aguirre
Farmacologicos Veterinarios S.A.C. FARVET
Manuel Criollo-Orozco
Farmacologicos Veterinarios S.A.C. FARVET
Edison Huaccachi-Gonzalez

Farmacologicos Veterinarios S.A.C. FARVET

Elmer Delgado-Ccancce
Farmacologicos Veterinarios S.A.C. FARVET

Doris Villanueva-Pérez
Farmacologicos Veterinarios S.A.C. FARVET

Ricardo Montesinos-Millan
Farmacologicos Veterinarios S.A.C. FARVET

Kristel Gutiérrez-Manchay
Farmacologicos Veterinarios S.A.C. FARVET

Katherine Pauyac-Antezana
Farmacologicos Veterinarios S.A.C. FARVET

Ingrid Ramirez-Ortiz
Farmacologicos Veterinarios S.A.C. FARVET

Stefany Quiñones-Garcia
Farmacologicos Veterinarios S.A.C. FARVET

Yudith Cauna-Orocollo
Farmacologicos Veterinarios S.A.C. FARVET

Katherine Vallejos-Sánchez
Farmacologicos Veterinarios S.A.C. FARVET

Angela Rios-Angulo
Farmacologicos Veterinarios S.A.C. FARVET

Dennis Núñez-Fernández
Farmacologicos Veterinarios S.A.C. FARVET

Mario I. Salguedo-Bohorquez
Farmacologicos Veterinarios S.A.C. FARVET

Julio Ticona
Farmacologicos Veterinarios S.A.C. FARVET

Manolo Fernández-Sánchez
Farmacologicos Veterinarios S.A.C. FARVET

Eliana Icochea
Farmacologicos Veterinarios S.A.C. FARVET

Luis Guevara-Sarmiento
Farmacologicos Veterinarios S.A.C. FARVET

Mirko Zimic (mirko.zimic@farvet.com)
Farmacologicos Veterinarios S.A.C. FARVET

COVID-19 Working Group in Perú.
Farmacologicos Veterinarios S.A.C. FARVET

Research Article

Keywords: SARS-CoV-2, COVID-19, Newcastle disease virus (NDV), neutralizing antibodies, vaccines, intranasal immunization, Spike protein subunit S1, receptor binding domain (RBD)

Posted Date: April 27th, 2021

DOI: https://doi.org/10.21203/rs.3.rs-420780/v1

Preclinical Evaluation of a Newcastle Disease Virus-Vectored Intranasal SARS-CoV-2 Vaccine

Manolo Fernandez Díaz[1*], Katherine Calderón[1], Aldo Rojas-Neyra[1], Vikram N. Vakharia[2], Ricardo Choque-Guevara[1], Angela Montalvan[1], Astrid Poma-Acevedo[1], Dora Rios-Matos[1], Andres Agurto-Arteaga[1], Maria de Grecia Cauti-Mendoza[1], Norma Perez-Martinez[1], Gisela Isasi-Rivas[1], Luis Tataje-Lavanda[1], Yacory Sernaque-Aguilar[1], Freddy Ygnacio-Aguirre[1], Manuel Criollo-Orozco[1], Edison Huaccachi-Gonzalez[1], Elmer Delgado-Ccancce[1], Doris Villanueva-Pérez[1], Ricardo Montesinos-Millan[1], Kristel Gutiérrez-Manchay[1], Katherine Pauyac-Antezana[1], Ingrid RamirezOrtiz[1], Stefany Quiñones-Garcia[1], Yudith Cauna-Orocollo[1], Katherine Vallejos-Sánchez[1], Angela A. Rios-Angulo[1], Dennis Núñez-Fernández[1], Mario I. Salguedo-Bohorquez[1], Julio Ticona[1], Manolo Fernández-Sánchez[1], Eliana Icochea[1,3], Luis Guevara-Sarmiento[1], Mirko Zimic[1*], COVID-19 Working Group in Perú.

[1] Farmacológicos Veterinarios S.A.C. FARVET

[2] Institute of Marine and Environmental Technology, University of Maryland Baltimore County, Baltimore, USA

[3]Laboratorio de Patología Aviar. Facultad de Medicina Veterinaria. Universidad Nacional Mayor de San Marcos, Lima, Perú

* Corresponding authors:

Email: Farvet@farvet.com. Panamericana Sur N° 766 Km 198.5. Chincha Alta, Ica, Perú.

Email: mirko.zimic@farvet.com. Panamericana Sur N° 766 Km 198.5. Chincha Alta, Ica, Perú.

ABSTRACT

The COVID-19 pandemic has claimed the lives of millions of people. Vaccination is a critical tool for the control of transmission; however, the recent emergence of potentially vaccine-resistant variants renders it important to have a range of vaccines types. It is desirable that vaccines are safe, effective, easy to administer and store, and inexpensive to produce. Newcastle disease virus (NDV), responsible for respiratory disease in chickens, has no pathogenic homologue in humans. We developed two types of NDV-vectored candidate vaccines, and evaluated them in a SARS-CoV-2 challenge in hamsters. Vaccinations resulted in generation of neutralizing antibodies, prevented lung damage, and reduced viral load and viability. In conclusion, our NDV-based vaccine candidate performed well in a SARS-CoV-2 challenge and warrants evaluation in a Phase I human clinical trial. This candidate represents a promising tool in the fight against COVID-19.

KEY WORDS: SARS-CoV-2, COVID-19, Newcastle disease virus (NDV), neutralizing antibodies, vaccines, intranasal immunization, Spike protein subunit S1, receptor binding domain (RBD)

INTRODUCTION

The severe acute respiratory syndrome coronavirus 2 (SARS-CoV-2) recognizes the angiotensin-2 converting enzyme (ACE-2), present on the surface of several human cell types including pneumocytes. The glycosylated Spike (S) protein gives the virus the ability to bind to the cell membrane and promote endocytosis, allowing entry of the viral particle [1,2]. The Spike protein is comprised of two subunits, S1 and S2. The most distal end of the S1 subunit is the receptor binding domain (RBD), which interacts with ACE-2 through the receptor binding motif (RBM) [3]. Previous studies with SARS-CoV and Middle Eastern respiratory syndrome coronavirus (MERSCoV) have helped to identify potential SARS-CoV-2 vaccine candidates, particularly encompassing the S protein due to its known immunogenicity [4–7]. SARS-CoV-2 has also been found to have potential B and T lymphocyte protective epitopes with the potential for vaccine candidate [8,9]. The S1 and RBD domains are considered important vaccine targets [10] and have been the focus of vaccine development to date. However, the amino acid sequences of S1/RBD are found to be under a selection pressure, seeking a greater affinity for ACE-2 [11–15] or escape from neutralization by antibodies against S1 of SARS-CoV-2 [16,17]. Different strategies have been applied for the development of vaccines against SARS-CoV-2, seeking safety, effectiveness and protection against the virus, including vaccines based on inactivated virus, those based on mRNA, and those using viral vectors [18–21].

Newcastle disease virus (NDV), the causative agent of the Newcastle disease (ND), has been used as a viral vector for the expression of diverse antigens from animal and human pathogens [22–24]. NDV is a member of the *Paramyxoviridae* family, recently known as *Avian orthoavulavirus 1* [25].

NDV is a single-stranded, negative-sense RNA virus with a genome size of approximately 15.2 kb [26,27]. NDV encodes six structural proteins: nucleocapsid protein (NP), phosphoprotein (P), matrix protein (M), fusion protein (F), haemagglutinin–neuraminidase protein (HN), and the large protein (L), which is a viral polymerase [26,27].

NDV can be divided into three groups according to their virulence in poultry: velogenic, mesogenic, and lentogenic [26]. NDV strain LaSota is lentogenic, and it is routinely used as a live NDV vaccine. It grows to a high titer in embryonated chicken eggs, induces strong humoral and cellular immune responses, and can be administered via the nasal route [27].

It has been demonstrated in prior studies that NDV does not pose a threat to human health, and the majority of the human population does not have pre-existing immunity [23,28,29]. NDV has selectivity for tumors, acting as an oncolytic virus. Tumoral cell defects, including anti-viral and apoptotic pathways [30], explain the NDV-mediated oncolytic efficiency in mammal cells, through manipulation of antiviral cellular pathways, induction of apoptosis, and indirect activation of the innate and adaptive immune response (humoral, cellular, and mucosal) [22,31,32].

NDV has been used as a vector for vaccine development since the late 1990s. The efficiency of vaccines based on this vector has been demonstrated against respiratory viruses, in chickens against infectious bronchitis virus and avian reovirus, in monkeys against SARS-CoV and in camels against MERS-CoV [33-36]. These studies have demonstrated that it is feasible to produce S protein from other viruses, especially of SARS-CoV and MERS, which conferred strong immunogenicity and protection in mice and non-humans primates [35,36]. Recently, NDV has been proposed as a potential vector for a vaccine against SARS-CoV-2. Sun, *et al.* demonstrated in vivo that a NDV-vectored vaccine against SARS-CoV-2 administered by the intramuscular route induces a high immune response in mice and hamsters, including reduced weight loss and decreased viral load in the lungs of challenged animals [37,38]. Of note, NDV-vectored vaccines induce mucosal immune response at the respiratory tract, and do not recombine with host DNA during replication [35].

In this study, we describe the design and evaluation of an intranasal NDV-vectored vaccine in hamsters challenged with SARS-CoV-2. The S1 and RBD domains of SARS-CoV-2 spike protein were expressed independently on the surface of a recombinant NDV.

RESULTS

Development and characterization of recombinant NDV expressing SARS-CoV-2 RBD and S1 antigens

Generation of rNDVs expressing RBD and S1 subunit genes of SARS-CoV-2

Vero-E6 cells were co-transfected with full-length plasmid cDNA of constructs pFLC-LS1-HNRBD and pFLC-LS1-S1-F together with three supporting plasmids encoding the NP, P, and L proteins of NDV, essential for the replication of NDV (Figure 1A, 1B). At 72 h post-transfection, the cells showed several visible plaques with typical cytopathic effect (CPE) from NDV, demonstrating the successful rescue of both recombinant viruses. Supernatants collected five days after transfection were injected into allantoic cavities of 9 day old embryonated specific pathogen free (SPF eggs). The allantoic fluid was harvested four days after inoculation and analyzed by hemagglutination (HA) assays using chicken red blood cells. We found positive HA titers ranging from 2 to 2048.

The presence of the HN-RBD and S1-F expression cassettes inserted into the non-coding region between the P and M genes of the NDV genome was verified by RT-PCR, yielding fragments of 1600 and 3028 bases pairs (bp), which were subsequently amplified and sequenced using junction primers NDV-3LS1-2020-F1 and NDV-3LS1-2020-R1, demonstrating proper insertion into the NDV genome (Figure 1C). The new recombinant NDV viruses were named rLS1-HN-RBD and rLS1-S1-F, respectively.

Expression of the SARS-CoV-2 Proteins in rLS1-HN-RBD and rLS1-S1-F Viruses. Two protein bands with a molecular mass of ~90 kDa (S1-F) and ~30 kDa (HN-RBD) were detected in cell lysates infected with rLS1-S1-F and rLS1-HN-RBD viruses respectively (Figure 2A). Two protein bands were detected in the purified recombinant virus (Figure 2B), confirming that the S1-F or HN-RBD proteins were incorporated into the viral particles of rLS1-S1-F and rLS1-HN-RBD viruses respectively. These protein bands were not detected in the rLS1-infected cells or in purified viral particles from the rLS1 virus.

The expression of the SARS-CoV-2 RBD and S1 subunit was detected in Vero-E6 cells infected with rLS1-HN-RBD, and rLS1-S1-F by Immunofluorescence assay. RBD and S1 subunit expression was not detected in cells infected with the rLS1 virus. NDV protein expression was detected using a chicken antiserum specific to NDV, and a Goat Anti-Chicken IgY H&L-Alexa Fluor 488 in Vero-E6 cells infected with rLS1, rLS1-HN-RBD, and rLS1-S1-F viruses (Figure 2C).
Detection of SARS-CoV-2 S1 subunit or RBD on the viral surface of rLS1-S1-F and rLS1-HNRBD viruses bound to Vero E6 cells was confirmed by flow cytometry in two independent experiments (Figure 2D). For the rLS1-S1-F virus, 40.4% positive cells were detected, for the rLS1HN-RBD virus 10.2% positive cells were detected, and for the rLS1 virus up to 0.37% positive cells were detected. A higher percentage of cells was detected in the rLS1-S1-F virus than the rLS1-HNRBD virus.

Immunogenicity in hamsters

Intranasal vaccination elicits specific antibodies against S protein and neutralizing antibodies against SARS-CoV-2 in hamsters

Fifteen days after prime immunization, the hamster groups immunized with the live rLS1-HN-RBD, rLS1-S1-F, and the combined rLS1-HN-RBD/rLS1-S1-F vaccines developed specific serum IgG antibodies against S1 and RBD (Figure 3A). At 15 days post-boost (30 days post-immunization) there was a significant increase in the titers of serum IgG antibodies. The control group did not induce SARS-CoV-2 S1 or RBD-specific serum IgG antibodies. Immunization with rLS1-S1-F induced a significantly higher level of S1 and RBD-specific serum IgG antibodies at 15 days postboost when compared to rLS1-HN-RBD and the combined of rLS1-HN-RBD/rLS1-S1-F vaccines (Figure 3B-3C).
Neutralization assays using the surrogate virus neutralization test (sVNT) indicated that the sera of groups immunized with rLS1-HN-RBD, rLS1-S1-F, and rLS1-HN-RBD/rLS1-S1-F developed neutralizing antibodies specific to RBD protein at 15 days post-immunization and 15 days postboost. However, the sera from hamsters vaccinated with rLS1-S1-F and rLS1-HN-RBD/rLS1-S1-F showed a percentage of inhibition of the RBD-ACE2 binding greater than 50% whereas the LS1HN-RBD group only showed

30% inhibition up to 15 days post-boost. Sera of the control group remained below 20% up to 15 days post-boost and did not show neutralizing antibodies against the RBD protein (Figure 3D).

Pooled serum from hamsters vaccinated with the rLS1-S1-F virus showed a strong titer of viral plaque reduction in the neutralization assay (PRNT) at 15 days post-boost, retaining 100% of this capacity even at higher dilutions of serum (1/160). The combined rLS1-HN-RBD/rLS1-S1-F vaccine showed a lower titer of viral plaque reduction (1/40), and rLS1-HN-RBD had no effect on viral plaque formation (Figure 3E-3F).

Cellular immunity: Cytokines quantification by ELISA

Immunization of hamsters did not induce a significant increase in serum levels of IL-2 or IFNγ, evaluated by quantitative ELISA. Levels of IL-2 (Figure 4A) did not show a significant increase with rLS1-HN-RBD (P = 0.55), rLS1-S1-F (P = 0.07) or rLS1-HN-RBD/rLS1-S1-F (P = 0.07). However, one of the individuals analyzed which had been vaccinated with rLS1-HN-RBD/rLS1-S1F had high levels of circulating IL-2. Levels of IFNγ (Figure 4B) did not increase significantly with rLS1-HN-RBD (P = 0.08), rLS1-S1-F (P = 1.00) or rLS1-HN-RBD/rLS1-S1-F (P = 0.56). Levels of IL-4 and IL-10 were below the lower limit of detection, and for TNFα values were low and were detectable only in serum from animals immunized with rLS1-S1-F and rLS1-HN-RBD/rLS1-S1-F (Supplementary Figure 1).

Cellular immunity: Cytokines quantification by qPCR

No significant difference in cytokine gene expression was observed for any of the vaccines used (Figure 4C-4D-4E): for rLS1-HN-RBD (IFNγ 1.2-fold, P=1.00, TNFα 1.48-fold, P=0.16, IL-10 1.7fold, P=0.16), rLS1-S1-F (IFNγ 1.16-fold, P=0.16, TNFα 1.48-fold, P=0.14, IL-10 P=0.16) or rLS1HN-RBD + rLS1-S1-F (IFNγ 0.81-fold, P=0.48, TNFα 1.12-fold, P=0.48, IL-10 0.90, P=0.48).

Efficacy of the vaccines against SARS-CoV-2 challenge

On days 2 and 5 post-challenge with the SARS-CoV-2, a positive SARS-CoV-2 isolate was obtained from 100% of the unvaccinated control group in Vero cell culture, and by day 10 none of the hamsters had a positive isolate. Viral isolation and IFA showed that rLS1-S1-F and the combined rLS1-S1-F/rLS1-HN-RBD vaccine elicited good responses, with no virus isolated from any of the vaccinated hamsters and negative IFA detection in the lung tissue at days 5 and 10 postchallenge. The rLS1-HN-RBD vaccine alone did not demonstrate sufficient neutralizing capacity to prevent the infection: virus isolates were obtained at day 5 post-challenge, confirmed by IFA in lung tissue, in 100% of the hamsters that received this vaccine (Figure 5A).

Viral quantification by RT-qPCR of the viral isolate obtained from hamster lung homogenates grown in Vero cells confirmed the presence of a high viral load (Ctp: 12) in unimmunized (control) hamsters and hamsters immunized with the rLS1-HN-RBD and rLS1-HN-RBD/rLS1-S1-F vaccines at day 2 post-challenge. Animals immunized with rLS1-S1-F showed a lower viral load (Ctp: 25). At day 5 post-challenge, the viral load from the isolate was maintained in the control group and in hamsters immunized with rLS1-HN-RBD, however, in hamsters immunized with rLS1-S1-F and rLS1-HN-RBD/rLS1-S1-F the viral load decreased significantly (Ctp: 28-31, $P < 0.05$, Figure 5B). On day 10 post-challenge all of the groups analyzed, including the control, presented a low viral load (Ctp: 32-34) (Figure 5B), probably due to the presence of residual RNA, since we did not detect any cytopathic effect on Vero cell culture.

The histopathological status of the hamster lungs was monitored during the SARS-CoV-2 challenge. The unvaccinated (control) group demonstrated pathological signs of the disease, starting with interstitial pneumonia at 2 days post-challenge, evolving into hemorrhagic pneumonia at 5 days post-challenge, and ending up in severe bronchopneumonia, characterized by a thickening in the parenchyma wall, greater infiltration of inflammatory cells, and in bronchioles lumen, and loss of alveolar architecture. The groups immunized with rLS1-S1-F and rLS1-HN-RBD/rLS1-S1-F vaccines did not show visible lesions, maintaining characteristics of the lung tissue similar to those seen in the unchallenged group at each of the evaluated points. However, the group immunized with rLS1-HN-RBD vaccine developed pathology that was less severe than that seen in the unvaccinated group, with pneumonia present at 2 days post-challenge and ending in a moderate to severe pneumonia at 10 days (Figure 5C).

Unvaccinated animals belonging to the unchallenged control group showed an average percentage variation in body weight of no more than 3% over the 10 days of analysis. Unvaccinated animals that were infected with SARS-CoV-2 showed significant weight loss, with an average reduction in body weight of over 5% on day 5 and over 10-25% on day 10. There were no statistically significant differences between the weight of vaccinated and unvaccinated, unchallenged hamsters on days 2 and 5, but there was a significant difference between the challenged control group and the rLS1-HN-RBD/rLS1-S1-F vaccinated group at day 10 (Figure 6A).

Assessments of the animals' average speed, acceleration, and displacement confirmed that hamsters vaccinated with the combined rLS1-S1-F/rLS1-HN-RBD vaccine were the most mobile on day 5 (time at which symptoms appear) and day 10 (time at which symptoms disappear) post-challenge. Animals vaccinated with the combined rLS1-S1-F/rLS1-HN-RBD vaccine showed the greatest recovery in terms of mobility (Figure 6B-6C-6D).

DISCUSSION

In this study, we developed two recombinant NDV nasal vaccine candidates expressing the SARSCoV-2 S1 and RBD antigens. The vaccine candidate expressing S1 showed favorable results during its evaluation in the pre-clinical phase.

Efficacy assessment in hamsters showed that the vaccine was able to effectively protect the animals against the SARS-CoV-2 targets, S1 and RBD antigens: the lungs of vaccinated animals did not show any evidence of cell damage, and the viral load as well as viral viability were considerably lower in the vaccinated group compared to the control group. In keeping with these results, the vaccinated animals showed significantly greater mobility than the control group, and showed no evidence of weight loss, in contrast to what was observed in the control group. Together with these encouraging results, that this is a nasal vaccine that is easy to administer, is lyophilized and stable in storage at 4°C, and is a relatively fast and economical vaccine to produce, make this vaccine candidate a promising tool to contribute to the fight against the pandemic.

The RBD domain, and in particular the RBM motif, are the regions of the spike protein that directly interact with the ACE2 receptor to initiate the infection process, and therefore constitute the most important target for neutralizing antibodies [39,40]. Recent studies have shown that in COVID-19 convalescent patients, neutralizing antibodies are commonly directed against specific epitopes of the RBD domain [39,40].

Three nasal vaccine candidates were evaluated in this study. One was an NDV presenting the RBD domain (rLS1-HN-RBD), the second was an NDV presenting the S1 subunit (rLS1-S1-F), which includes the RBD domain, and the third was a mixture of both rLS1-HN-RBD and rLS1-S1-F. The strongest immunity and protection were elicited by the rLS1-S1-F vaccine, followed by the combined rLS1-HN-RBD/ rLS1-S1-F vaccine. Surprisingly, the rLS1-HN-RBD vaccine did not show any evidence of protection. There are at least two possible explanations that are not necessarily mutually exclusive. First, the S1 subunit may include protective epitopes in addition to those present in the RBD domain, for which neutralizing antibodies could interfere with the SACE2 interaction perhaps at a distant steric level. This possibility is supported by a previous study that showed that the S1 subunit contains neutralizing epitopes not found in the RBD [41]. Second, the RBD present in the rLS1-HN-RBD vaccine does not reach folding close enough to the 3dimensional structure of the biologically active RBD when it is in the SARS-CoV-2 viral particle. It is likely that the presence of the additional S1 moiety may provide support for RBD to reach a more comparable folding. Therefore, it is possible that conformational B epitopes may be playing a more important role than linear T epitopes in the protective immune response. A recent study that evaluated a similar vaccine candidate vectored in NDV exposing the complete S antigen (S1 and S2

domains) demonstrated protection of hamsters in a challenge assay [38]. It is likely that the major contribution to the protection observed in these studies is associated with S1, which includes the RBD domain in a protein environment that favors the proper folding, allowing the presentation of appropriate conformational B epitopes.

Animals from the unvaccinated control group that were challenged with SARS-CoV-2 positive virus cultures at 2 and 5 days post challenge (dpc), which became negative at day 10. This is consistent with previous studies, which reported that viral load is reduced to undetectable levels by 8 days after infection in the hamster model [42,43]. Along with the culture results, the IFA test also confirmed that the rLS1-S1-F vaccine, followed by the combined rLS1-HN-RBD/ rLS1-S1-F vaccine, induced the strongest protective responses, evidenced by failure to isolate virus from the lung tissue at 5 dpc. At 2 dpc, only half of the animals vaccinated with the rLS1-S1-F vaccine had virus isolated, and these had a negative IFA. This suggests that inactivation of the inoculated SARS-CoV-2 virus is likely to be occurring between 2 and 3 dpc in the hamster model.

Histopathological evaluation of the non-vaccinated hamsters' lungs after the challenge showed severe pathological signs of the disease, beginning with interstitial pneumonia 2 dpc, evolving to hemorrhagic pneumonia, and ending in severe bronchopneumonia, as well as the loss of alveolar architecture. In contrast, the groups immunized with rLS1-S1-F and rLS1-HN-RBD/rLS1-S1-F were protected, showing almost intact alveoli, capillaries, and respiratory capillaries, without evidence of an inflammatory reaction. However, the animals vaccinated with rLS1-RBD-HN developed pathological lesions, although with a lesser hemorrhagic degree than the non-vaccinated control group, with pneumonia at 2 dpc and ending in a moderate to severe pneumonia at 10 dpc. Recent studies reported that Golden Syrian hamsters inoculated by the intranasal route with $8x10^4$ $TCID_{50}$ SARS-CoV-2 show efficient virus replication in the respiratory epithelium associated with a reduction in the number of replicating olfactory sensory neurons of the nasal mucosa at 2 dpc [43], however, virus clearance is observed from 7-10 dpc [42,43]. The ability of the rLS1-S1-F vaccine to neutralize the SARS-CoV-2 virus, block its replication in the cell culture between 2 and 5 dpc, and reduce its presence in the lungs according to the IFA assay, suggests that the rLS1-S1-F vaccine may reduce virus transmission from 2 dpc in the hamster model. This is an encouraging result that needs to be verified in human clinical trials.

In the hamster challenge trial, the animals in the non-vaccinated control group lost significant body weight (10-25%) during the 10-day trial period. Animals vaccinated with rLS1-S1-F showed a minor body weight variation similar to that of the uninfected (mock) group, suggesting a protective effect of this vaccine candidate.

In this study, we evaluated for the first time the mobility pattern of the animals as an objective and quantitative indicator of their health status. Using recorded videos and computational tools for pattern analysis and digital tracking, we measured the average velocity, the average acceleration, and the average displacement of the animals in their cages at 2, 5, and 10 dpc. The results showed that at 5 dpc, the animals from the unvaccinated control group had a reduced average displacement, velocity, and acceleration compared to the vaccinated animals. This marked difference was not clearly observed at 2 dpc, confirming that at that time point, the infected animals may have been relatively asymptomatic. Similarly, at 10 dpc all animals recovered their mobility with no differences observed.

This result agrees with other findings that show clearance of the virus at 10 dpc.
A favorable result that suggests strong protection of the rLS1-S1-F vaccine is the neutralization capacity of the vaccinated hamsters' sera against the SARS-CoV-2 virus at 30 days after immunization in the PRNT test. In contrast, animals vaccinated with rLS1-HN-RBD showed marginal sero-neutralization capacity. This result agrees with similar findings reported in a recent study evaluating an intranasal NDV-vectored live attenuated SAS-CoV-2 vaccine, showing that humoral immunity is induced to high levels in a relatively short time [44].

Respiratory viruses induce a strong response in the respiratory tract mucosa, so vaccines based on the NDV vector should be effective in respiratory diseases and reduce transmission. Likewise, a vaccine candidate for SARS-CoV based on the NDV construct using the S protein confirmed that two doses 28 days apart of 10^7 PFU delivered by the intranasal and intratracheal routes produced significant protection against SARS-CoV in juvenile primates *Cercopithecus aethiops* [35]. In a recent study, an NDV-vectored nasal vaccine displaying the S protein was able to induce an IgA antibodymediated mucosal humoral response [44]. A mucosal antibody response is considered important against infections that use the respiratory tract as a route of entry, making the respiratory tract mucosa the first line of defense against this infection. Currently, we are completing an assay to evaluate the presence of anti-S1/RBD mucosal IgA antibodies in mice vaccinated with rLS1-S1-F. Preliminary data show evidence of IgA production in bone marrow cells (data not shown). Further studies are required to confirm this finding.

Other studies have reported that NDV virus is restricted to the respiratory tract and is not detected in other organs or blood, therefore replication in humans is expected to be limited and benign [45,46]. Rarely, humans exposed to mesogenic NDV have been observed to develop conjunctivitis, laryngitis, or flu-like symptoms that disappear within 1 to 2 days [46,47]. Crucially, safety and toxicity tests were conducted with doses that were not produced under strict GMP certification. That the trials were conducted with non GMP doses of the vaccine means that any adverse events will be over-projected, and lower rates would be expected in an evaluation of the vaccine at doses produced under GMP conditions.

NDV has been repeatedly used in the development of successful vaccines to eliminate infectious diseases in poultry [27]. Currently, there is an NDV strain genotype XII that predominates in Peru, China and Vietnam, which has been used to develop rNDV vaccines [48]. Likewise, Shirvani *et al.* used the rNDV vector to control infectious bronchitis in free-range chickens, in which the spike S protein is expressed, showing equal efficacy as the same infectious bronchitis virus vaccine [33]. The LaSota is the attenuated NDV strain most commonly used as a vaccine around the world against NDV infection, with doses of $TCID_{50}$ ranging from 10^4 to 10^5 and which is administered to animals by oral, nasal, ocular, or spray delivery [49–51]. This results in frequent exposure of vaccinators to NDV virus, which ends up being inhaled. Thus, vaccinators and caretakers are frequently exposed to the NDV vector without any reported side effects to date [52–54]. Accumulated doses of NDV inhaled by vaccinators in Chincha-Peru over the last few decades have never resulted in any reported adverse effects in this population (data not shown).

The development of the NDV-vectored vaccine candidate presented here includes a final lyophilization step. This confers stability: the vaccine can be stored at 8°C for several months without losing more than 5% of its activity, similar to other lyophilized vaccines [55]. The fact that the NDV-S1 vaccine is administered through the nasal route gives it a further advantage in simplifying the logistical requirements for immunizations. There is no need for an army of vaccinators or large numbers of syringes. It is possible that doses of rLS1-S1-F vaccine could be delivered in 500-dose vials with a manual trigger-activated dispenser system that uses individual disposable tips. In this way, a nasal vaccine could be delivered in large-scale campaigns in remote rural communities with great ease.

The COVID-19 pandemic has the potential to become endemic, and if this were to happen vaccines would need to be routinely administered with some frequency [56,57]. SARS-CoV-2 in recent months has shown an intense level of mutations in the viral antigens used in the various vaccines currently available. These mutations have been selected naturally, in the face of the immunological pressure exerted by individuals cured of COVID-19. Thus, mutations have now been identified that may give the virus the ability to escape acquired immunity (immune resistance), and this may lead to a surge in cases of SARS-CoV-2 reinfection. These same naturally selected mutations have also been selected *in vitro*, under immunological selection pressures using convalescent serum neutralizing antibodies.

This suggests a high possibility that vaccines based on circulating S1 antigen in the early 2020's may be compromised to some degree in their level of effectiveness against new SARS-CoV-2 variants. Therefore, the most efficient way to deal with the COVID-19 pandemic will be to use vaccines customized for specific geographic areas, based on the distribution of circulating variants over a certain period of time, and which can be produced and administered promptly. The rLS1-S1F vaccine can be upgraded and carry a vaccine antigen corresponding to a more relevant strain in a relatively short time.

NDV can be transformed within 30-45 days, and a master cryobank generated to start producing updated vaccine batches. It is therefore important to have permanent epidemiological surveillance programs to identify any variation in the distribution of circulating strains in a region of interest.

In conclusion, we have demonstrated that our rLS1-S1-F vaccine candidate shows promise in preclinical studies. This vaccine candidate was shown to be safe and immunogenic, and provided strong protection against a SARS-CoV-2 challenge. Clinical trials are now needed to evaluate its safety and efficacy in humans.

METHODS

Ethics statements

Animal research was conducted following relevant guidelines and regulations. All experimental protocols were approved by the Bioethics Committee of the Universidad Nacional Hermilio Valdizán, Huánuco, Peru. The study was carried out in compliance with the ARRIVE guidelines.

SARS-CoV-2 (28549) virus used in the challenge was provided by the National Institute of Health (INS), Lima, Peru, in accordance with relevant guidelines and regulations. The isolation of the SARS-CoV-2 virus was approved by the General Direction of the Public Health Centre of the INS.

Animals

One hundred male and female Golden Syrian hamsters (*Mesocricetus auratus*) aged 4-5 weeks were obtained from the Peruvian National Institute of Health (INS). For the in-vivo assay, all hamsters were transferred and acclimatized to the Animal Biosafety Level 3 (BSL-3) facility for 1 week. There, they were vaccinated with NDV-vectored SARS-CoV-2 vaccine and later challenged with live SARS-CoV-2.

Development and characterization of recombinant NDV expressing SARS-CoV-2 RBD and S1 antigens

Cell Culture

African green monkey kidney cells, clone E6 (Vero E6, ATCC® CRL-1586™) and DF-1 cells (derived from Chicken Fibroblast), were maintained in Dulbecco's modified Eagle's medium (DMEM), supplemented with 5% heat-inactivated fetal bovine serum (FBS) (HyClone™ GE Healthcare Life Science, USA). Vero cells (Vero 81, ATCC® CCL-81™) were grown in Eagle's Minimum Essential Medium (EMEM) supplemented with 10% FBS, 100 IU/mL of penicillin, and 100 µg/mL streptomycin. All cell lines were cultivated at 37°C in an atmosphere of 5% CO_2.

Plasmid Construction

Our vaccine candidates are based on the recombinant lentogenic NDV strain LaSota, which was designated the rLS1 virus. The design and construction of a pFLC-LS1 plasmid (19,319 nucleotides (nt)) containing the full-length genome of an infectious NDV clone, and the three support plasmids containing the N, P, and L genes (pCI-N, pCI-P, and pCI-L, respectively) have been previously described [58]. This NDV-based system is protected under a Peruvian patent 001179-2014/DIN.

The genetic sequences of the RBD and the S1 subunit of the S protein correspond to the SARSCoV-2 strain isolate from China *(*GenBank accession no. MN908947.3). To improve the incorporation of RBD and S1 into the NDV virion, we designed two cassettes. First, the HN-RBD transcriptional cassette (1,013 nt) contained the genetic sequences of the RBD (636 nt), followed by complete transmembrane domain (TM), and cytoplasmic tail (CT) of the NDV haemagglutinin– neuraminidase (HN) gene. Second, the S1-F transcriptional cassette (2,441 nt), which contained the genetic sequence of the S1 subunit (2,043 nt), taken from the S gene (3,822 nt). This sequence was fused with the TM and CT of the fusion (F) gene. These TM and CT gene sequences of HN and F genes were obtained from the pFLC-LS1 plasmid. Both transcriptional cassettes were flanked with specific gene-end (GE) and gene-start (GS) transcriptional signals of the paramyxovirus genome [59]. Further, these cassettes, flanked with restriction sites of *BbvCI,* were chemically synthesized and were subsequently cloned into plasmid pUC57 by GenScript (Piscataway, NJ, USA). These plasmids were purified and DNA extracted using QIAGEN Plasmid Midi Kit (100), according to the manufacturer's instructions.

The pFLC-LS1 plasmid, containing a unique *BbvCI* site, was digested with *BbvCI* enzyme to obtain the linearized plasmid. Both the HN-RBD and S1-F transcriptional cassettes were digested with the same enzyme and inserted into the P/M junction of the pFLC-LS1 to be expressed as a separate mRNA. The resulting plasmids were designated as pFLC-LS1-HN-RBD (20,315 nt) and pFLCLS1-S1-F (21,743 nt).

Recovery of the rLS1-HN-RBD and rLS1-S1-F virus

Briefly, the rLS1-HN-RBD and rLS1-S1-F viruses were recovered by co-transfection with a fulllength plasmid complementary DNA (cDNA) of each construct, pFLC-LS1-S1-F and pFLC-LS1HN-RBD, respectively, together with three support plasmids, as described previously [58]. The recovered viruses were injected into the allantoic cavities of 9 day old SPF embryonated chicken eggs (Charles River, Norwich, CT, USA). After incubation for four days at 37°C, the allantoic fluid containing the recovered virus were harvested, clarified, aliquoted and stored at -80°C. The presence and recovery of viruses were confirmed by hemagglutination (HA) assays using 1% chicken red blood cells. The identity of the recombinant viruses was confirmed by reverse transcription-polymerase chain reaction (RT-PCR) and by Sanger sequencing, as described before

[48].

Indirect Immunofluorescence Assay (IFA)

To examine the SARS-CoV-2 S RBD and S1 subunit proteins expression, Vero-E6 cells were infected with the recombinant rLS1-HN-RBD, rLS1-S1-F and rLS1 viruses at a multiplicity of infection (MOI) of 0.5. After 48 hours post-infection (hpi), the cells were fixed with 4% paraformaldehyde for 25 minutes (min), and then the monolayer was washed three times with Dulbecco's phosphate-buffered saline (DPBS) and permeabilized with Triton 0.1% X-100 for 15 min at room temperature (RT). After washing with the cells with DPBS, the monolayer was incubated with the rabbit polyclonal antibody specific to SARS-CoV-2 RBD protein (1:200) (Sino Biological, Beijing, China), and a chicken antiserum specific to Newcastle disease virus (1:200)
(Charles River, Norwich, CT, USA) for 1.5 h at RT. Afterwards, the monolayer was incubated with Donkey Anti-Rabbit IgG H&L-Alexa Fluor® 594 (1:250) and Goat Anti-Chicken IgY H&L-Alexa Fluor® 488 (1:1000) (Abcam, Cambridge, MA, USA) for 60 min at RT. Finally, the cells were developed with 4′,6-diamidino-2-phenylindole (DAPI) for 5 min and observed using an ObserverA1 fluorescence microscope (Carl Zeiss, Germany). Digital images were taken at 400 X magnification and processed with the AxioCam MRc5 camera (Carl Zeiss, Germany).

Western Blot Analysis

To evaluate the SARS-CoV-2 RBD and S1 subunit proteins expression, Vero E6 cells were infected with the recombinant viruses mentioned above at an MOI of 1. At 48 hpi, the cells were harvested, lysed, and analyzed by Western blot. Additionally, to verify the incorporation of the RBD and S1 subunit proteins into rLS1-HN-RBD and rLS1-S1-F viruses, viral particles from allantoic fluid of SPF chicken embryonated eggs infected with the recombinant viruses and rLS1, were concentrated by ultracentrifugation (Ultracentrifuge, Beckman, Coulter) at 18,000 revolutions per minute (rpm) at 4°C, and partially purified on a 25% sucrose cushion. Western blot analysis was carried out using partially purified viruses from allantoic fluid and lysate from infected cells, using a rabbit polyclonal antibody specific to SARS-CoV-2 RBD protein (Sino Biological, Beijing, China) (2/5000) as the primary antibody and anti-Rabbit IgG conjugated to HRP (GenScript, Piscataway, NJ, USA) (2/5000) as a secondary antibody. The protein expression was visualized with a CCD camera Azure c600 imaging system (Azure Biosystems, Dublin, USA).

Detection of RBD and S1 subunit proteins on the viral surface by flow cytometry

To determine the presence of RBD on the viral surface of rLS1-HN-RBD, and the presence of the

S1 subunit on rLS1-S1-F viruses, virion particles were purified with a 25% sucrose cushion. Vero E6 cells were harvested and washed with DPBS with 5% FBS. Approximately, $1x10^6$ cells were blocked with DPBS with 5% of normal mouse serum for 30 min at 37°C. Then, the cells were incubated with rLS1 (0.36 mg/mL), rLS1-S1-F (0.09 mg/mL) or rLS1-HN-RBD (0.2 mg/mL) purified viruses for 30 min at 37°C. To remove the residual viral particles not attached to Vero E6, the cells were washed with DPBS and 5% FBS twice. Subsequently, the mix was marked with rabbit monoclonal antibody anti-SARS-CoV-2 S1 (1:200) (Sino Biological, Beijing, China) as primary antibody for 1h at 37°C, followed by goat anti-rabbit IgG Alexa Fluor® 488 (1:200) (Abcam, Cambridge, MA, USA) as secondary antibody. Finally, the cells were analyzed in FACS Canto II (BD Biosciences, USA) flow cytometer. The data obtained were analyzed using the software FlowJo v.10.6 (BD Biosciences, USA), where the percentage of positive cells was taken to indicate detection of the SARS-CoV-2 S1 subunit or RBD on the viral surface of viruses bound to Vero E6.

Detection of RBD and S1 subunit genes by RT-PCR

For the detection of rLS1-HN-RBD and rLS1-S1-F recombinant virus, viral RNA was extracted from allantoic fluid stocks using the QIAamp MinElute Virus Spin kit. Complementary cDNA was generated from RNA using ProtoScript II cDNA Synthesis kit (New England Biolabs, USA), according to the manufacturer's instructions. The cDNA was amplified using the high-fidelity DNA polymerase Master Mix Q5 (New England Biolabs, USA), with the primers NDV-3LS1-2020-F1 (5´- GATCATGTCACGCCCAATGC-3 ') and NDV-3LS1-2020-R1 (5'-GCATCGCAGCGGAAAGTAAC-3') to amplify the complete inserts. The thermal cycling protocol comprised an initial denaturation step at 98°C for 30 seconds (s), followed by 35 cycles of 98°C for 10 s, 72°C for 20 s, 72°C for 30 s for the detection of rLS1-HN-RBD**,** and 40 s for the detection of rLS1-S1-F. The final extension step was at 72°C for 2 min.

Genetic stability of the rLS1-HN-RBD and rLS1-S1-F virus

The genetic stability of the recombinant viruses across multiples passages was evaluated on 9 day old SPF embryonated chicken eggs, the viral RNA was extracted from purified viruses of the 3rd and 6th passage, and the presence of the gene inserts was confirmed by RT-PCR using specific primers. The expression of the SARS-CoV-2 S1 subunit and RBD inserts was also evaluated using purified viruses of the 3rd and 6th passage by Western blotting.

In vitro replication properties of the rLS1-HN-RBD and rLS1-S1-F viruses, plaque assay, and pathogenicity

We compared the infectivity and growth properties between the rLS1-HN-RBD, rLS1-S1-F, and rLS1 viruses. The monolayer culture of DF-1 cells was seeded at 70% confluence in 12- well plates and infected with rLS1-HN-RBD, rLS1-S1-F, and rLS1 viruses at an MOI of 0.05. Cells were maintained with DMEM containing 1% FBS and 5% and incubated at 37°C with 5% CO_2. Supernatants of the infected cells were collected at 12, 24, 36, 48, 60, and 72 hpi and kept at -80°C. The titers of each collected supernatant were determined using plaque assay, as described previously [58]. These experiments were repeated at 3 specific time points. In addition, the morphology and size of the plaques of the two recombinant viruses were compared with those formed with rLS1 infection. To determine the pathogenicity, the viruses were evaluated by the Mean Death Time (MDT) and Intracerebral Pathogenicity Index (IPIC) assays in 10 day old SPF embryonated chicken eggs and one day old SPF chickens (Charles River Avian Vaccine Services, Norwich, CT, USA), respectively, using standard procedures [60].

Preparation and stability of the lyophilized vaccine

To check the stability of the lyophilized vaccine, the rLS1-RBD-HN and rLS1-S1-F viruses were separately inoculated into the allantoic cavities of 9 to 11 day old SPF embryonated chicken eggs. After four days of incubation at 37°C, the allantoic fluids were harvested, clarified, and filtered using 0.22 µm filters. The presence of the viruses in allantoic fluid was detected and confirmed by HA. Finally, the allantoic fluid containing the rLS1-RBD-HN, rLS1-S1-F, and the mixture of both viruses were placed in vials (2 mL/vial) and lyophilized using an MX5356 lyophilizer (Millrock Technology). The lyophilized vaccine of the mixture of rLS1-HN-RBD and rLS1-S1-F viruses were stored at 4°C and were evaluated by plaque assay, HA, and Western blot assays on days 1, 30, and 50 after lyophilization. The lyophilized vaccines were used in the following in vivo tests in hamsters.

Immunogenicity in hamsters

Forty-Eight Golden Syrian hamsters, weighing between 120-140 g, were divided into 4 groups (*n* =12 per group): group 1 (rLS1-HN-RBD), group 2 (rLS1-S1-F), group 3 (rLS1-HN-RBD/rLS1-S1F), and the unvaccinated control group 4, were intranasally immunized with $5x10^6$ PFU/hamster (40 µL volume) following a prime-boost regimen with a two-week interval. Immunized hamsters were bled immediately before the boost and fifteen days post-boost (at days 15 and 30 respectively), to measure the SARS-CoV-2 RBD and S specific serum IgG antibody by indirect ELISA assay, as well as the neutralizing antibody

519 (nAbs) titers using a surrogate Virus Neutralization Test (sVNT) and by Plaque Reduction Neutralization
520 Test (PRNT) against SARS-CoV-2 virus.

521 *Enzyme-Linked Immunosorbent Assay (ELISA) indirect IgG*

522 Immunized hamsters were bled on days 15 and 30 of the immunization. All sera were isolated by
523 centrifugation at 2500 rpm for 5 min. To perform the assay, Nunc MaxiSorp 96-well flat-bottom plates
524 were coated with 100 µL of SARS-CoV-2 RBD (1 µg/mL) and S1 subunit purified proteins (GenScript,
525 Piscataway, NJ, USA) dissolved in carbonate-bicarbonate buffer (pH 9.6) and incubated at 4°C
526 overnight. After coating the plates, standard ELISA protocol was followed as described earlier [48].

527 *Neutralization Tests using SARS-CoV-2 surrogate virus*

528 Serum samples were processed to evaluate nAbs titers against SARS-CoV-2. All neutralization assays
529 performed with the surrogate Virus Neutralization Test (sVNT) (GenScript, Piscataway, NJ,
530 USA), following the manufacturer's instructions. The positive and negative cut-offs for SARS-
531 CoV-2 nAbs detection were interpreted as inhibition rate, as follows: *positive*, if ≥ 20%
532 (neutralizing antibody detected), and *negative*, if <20% (neutralizing antibody no detectable).

533 *Plaque Reduction Neutralization Test (PRNT) of SARS-CoV-2 virus isolation of SARS-CoV-2* SARS-
534 CoV-2 (28549) was isolated from a nasopharyngeal swab sample collected from a patient with confirmed
535 SARS-CoV-2 infection in April 2020 in Lima, Peru. The identity of the virus was confirmed by whole
536 genome sequencing. Virus isolation was performed using Vero 81 cells maintained in Eagle´s Minimum
537 Essential Medium (EMEM) supplemented with 10% fetal bovine serum (FBS), 100 IU /mL of penicillin
538 and 100 µg/mL streptomycin and cultured at 37 °C in an incubator with humidified atmosphere at 5%
539 CO_2. The sample was filtered through a 0.22 µm pore membrane and inoculated with 100 µL into a
540 confluent monolayer of Vero 81 cell line. Cells were observed daily to detect the appearance of any
541 cytopathic effect and virus was collected for confirmation. The virus was propagated in Vero 81 cell
542 culture for viral stock production at -80°C and titer determined by PFU.

543 *Plaque Reduction Neutralization Test*
544 Pooled hamster serum samples were collected at day 30 of immunization and were heat-inactivated (HI)
545 at 56°C for 30 min. Then after two-fold serial dilutions, serum samples were mixed and incubated with
546 40-50 PFUs of SARS-CoV-2 (28549) for 1 h at 37°C in 5% CO_2. These serumSARS-CoV-2 mixtures
547 were added to Vero E6 cells (in 24-well plates) and incubated at 37°C for 1 h. After absorption, the
548 serum-virus mixtures were removed, and a liquid overlay medium (L-OM) comprising 0.75%
549 carboxymethylcellulose (CMC) (Sigma-Aldrich) supplemented with 2% FBS was added to the
550 monolayer cells, which were incubated at 37°C for 5 days. The plates were fixed and stained with 10 %

formaldehyde and 0.5% crystal violet solution [61]. Each serum sample was tested in duplicate. The plates were enumerated for the calculation of $PRNT_{50}$, considered the gold standard method [62].

Cellular immunity for Cytokines quantification by qPCR

Fifteen days post-immunization, spleens were collected from hamsters immunized with the different recombinant viruses and stored in RNAlater reagent at 4°C overnight and then at –80°C. RNA was extracted with RNeasy Mini kit, converted to cDNA with ProtoScript® II cDNA Synthesis kit, and stored at –20°C until analysis. Cytokines interferon-gamma (IFNγ), Tumor Necrosis Factor-Alpha (TNF-α) and interleukin-10 (IL-10), and reference gene β-actin were evaluated with primer pairs reported previously [63–66]. Standard curves were made for all primers, obtaining acceptable efficiency and R^2 values (data not shown). Master Mix preparation and cycling conditions were realized with Luna® Universal qPCR Master Mix kit (New England Biolabs), according to manufacturer's instructions. Briefly, five µL of the sample was used (~ 2 ng/µL cDNA) with 2-3 technical replicas.

The qPCR experiments were done on the Rotor-Gene Q equipment (Qiagen, Hilden, Germany) and the ΔΔCT method [67] was used for data analysis.

Cellular immunity for Cytokines quantification by ELISA

Fifteen days post-immunization, whole blood obtained from hamsters immunized with rLS1-HN-RBD, rLS1-S1-F, and rLS1-HN-RBD/rLS1-S1-F and allontoic fluid (mock) was centrifuged at 1000 x g for 20 min at 4°C to obtain the serum, which was duly aliquoted, frozen, and stored at 80°C until analysis. For the quantitative ELISA, several kits for the accurate quantitative detection of hamster's cytokines such as, TNFα, IFNγ, IL-2, IL-4, and IL-10 were purchased from MyBioSource, Inc., San Diego, CA. Cytokines quantifications were performed following the manufacturer's instructions. Briefly, the sera were added in 96-well plates (in duplicate) which were pre-coated with antibodies against the hamster's cytokines: TNFα, IFNγ, IL-2, IL-4, and IL-10. The sera were incubated at 37 °C and cytokines revealed with the enzyme streptavidin or avidin conjugated with peroxidase (HRP), giving a color by addition of the substrate 3, 3 ', 5, 5'tetramethylbenzidine (TMB). The plates were read in the EON spectrophotometer (Biotek, USA) at
450 nm. The level of cytokines (pg/mL) detected in the serum of the animals vaccinated with rLS1HN-RBD, rLS1-S1-F, and rLS1-HN-RBD/rLS1-S1-F were compared with mock animals.

Efficacy of the vaccines against SARS-CoV-2 challenge

Forty-eight golden Syrian hamsters, divided into 4 groups (n =12): group 1 (rLS1-HN-RBD), group 2 (rLS1-S1-F), group 3 (rLS1-HN-RBD/rLS1-S1-F), and the unvaccinated control group 4, were

intranasally challenged with 1 x 10^5 PFU/hamster in DMEM (40 µL volume) of SARS-CoV-2 at 45 days post-prime immunization. Four animals in each group were anesthetized and sacrificed with one overdose of 1mL of a mixture of Ketamine (100 mg), Xylazine (20 mg), and Atropine Sulfate (1 mg) by intramuscular injection at 2, 5, and 10 days post-challenge (dpc). The lung tissue samples (right and left lobes) were separated into two parts: (1) The right lobe was used for the pathological examination, and (2) the left lobe was immediately frozen at -80°C until used; this lobe was used for live infectious virus by viral isolation. SARS-CoV-2 (28549) virus used in the challenge was kindly provided by the National Institute of Health (INS), Lima, Peru. All work and handling with SARS-CoV-2 were performed in a BSL-3 laboratory following the biosafety guidelines of INS.

Histopathology analysis

Lungs obtained from sacrificed hamsters at days 2, 5, and 10 post-challenge with SARS-CoV-2 were fixed in 10% buffered formalin for 48 h. Organs were then reduced and placed in a container for 24 h with buffered formalin. The containers with the organs were processed in an automatic tissue processor (Microm brand) conducting the following processes: dehydration, diaphanating, rinsing, and impregnation within an 8 h. Organs embedded in paraffin were cut to a thickness of 5 microns (Microtome Leica RM2245 of disposable metal blades), placed in a flotation solution in a water bath and then fixed on a slide sheet, and dried in the stove (at 37°C for 1 to 2 h). The staining was done with the Hematoxylin and Eosin staining method (H&E) in a battery of staining bottles to remove paraffin, hydration, hematoxylin coloration, washing, Eosin coloration, rinsing, dehydration, drying, rinsing, and mounting in a microscope slide with Canada Balm (glue), and drying (at 37°C for 12 to 24 h) for further labeling. The final slides colored with H&E were taken and analyzed under an AxioCam MRc5 camera and AxioScope.A1 microscope (Carl Zeiss, Germany) at an amplitude of 20 and 40 x by a board-certified veterinary pathologist.

Viral viability: Culture and immunofluorescence assay (IFA)

For virus viability, 60 lung tissue samples from challenged animals were crushed and homogenized in 5 % w/v of DMEM 1% antibiotic, antimycotic and centrifuged at 10,000 rpm for 10 min at 4˚C. The supernatant was filtered with a 0.22 µm Millipore filter membrane, then 100 µL inoculated into a confluent monolayer of the Vero 81 cell line, and cultured at 37°C in an incubator with humidified atmosphere at 5% CO_2. The cultures were observed daily for 10 days through the inverted microscope. Lung virus isolation was confirmed by RT-PCR, as described previously [68]. The IFA was performed using a polyclonal antibody against SARS-CoV-2 from convalescent patients of COVID-19 disease, and anti-human IgG peroxidase conjugate (Sigma).

Animal mobility

To assess hamster's mobility (in groups 1 to 4) post-challenge, the average velocity, average acceleration, and average displacement were calculated based on videos with a camera positioned on top of the hamsters. The videos were analyzed on days 2, 5, and 10 post-challenge.

It should be noted that the conditions of video recording (distance and focus) were kept the same; therefore, the pixels always reflect the same distance. Since hamsters do not necessarily move a lot at the border of the box, we estimated average velocity, acceleration and displacement based on any movement that took place away from the edges the box (Supplementary Figure 2). Movement along the edges of the box were excluded and we tracked movement through a 2-3 min time period. After that, the hamsters were tracked in those time intervals where the hamster has no interaction with the edge of the box. Tracking was carried out using the Kernelized Correlation Filter (KCF) [69]. The implementation of this tracking algorithm was developed using the OpenCV library and the Python language. The result of tracking the hamsters was a record of the positions (X and Y) of the hamster in the image. Finally, once the tracking record was obtained at the intervals of interest, the average velocity, average acceleration, and average displacement were calculated for each of the hamsters.

Animal weight variation

The body weight change was measured on days 2, 5, and 10 post-challenge. An additional mock group (n=12) of unvaccinated and unchallenged animals outside the BSL3 were evaluated. These measurements were used to calculate the percentage of body weight variation, compared to day 0 for each animal.

Statistical analysis

For the statistical analysis of the weight variation in hamster groups, we used the one factor analysis of variance (ANOVA) in the statistical package Stata software v.16. For the comparison of treatments of the quantification of Cytokines, by qPCR and ELISA, we used the non-parametric Mann-Whitney-Wilcoxon test. Both tests were performed using the statistical software STATA v.16. To evaluate the statistical significance of body weight change in hamster groups, and a oneway ANOVA with multiple comparisons for all the treatments involved was performed in the software GraphPad Prism v.8.0.1. To evaluate changes in hamsters' mobility over time, nonparametric statistics using the Mann-Whitney and Kruskal-Walls tests were used SciPy v1.5.2 package. In all analyses, $P<0.05\%$ is considered statistically significant. To assess plaque reduction (%) of neutralization from the different groups of hamsters, we used two-way ANOVA and Tukey's post hoc in software GraphPad Prism v.8.0.1.

FIGURE LEGENDS

Figure 1. The strategy used for the generation of the recombinant NDVs expressing SARS-CoV-2 RBD and S1. (**A**) The schematic representation of the strategy of construction of the recombinant NDVs. Two transcriptional cassettes were designed for expressing RBD and S1: 1) HN-RBD was fused with the complete transmembrane domain (TM) and the cytoplasmic tail (CT) of the haemagglutinin–neuraminidase (HN) gene, 2) S1-F was fused with the TM/CT of the fusion (F) gene from the full-length pFLC-LS1. (**B**) The full-length antigenome of NDV strain LaSota clone (pFLC-LS1) was used as a backbone clone, the pFLC-LS1-HN-RBD and pFLC-LS1-S1-F were generated from cassettes expressing RBD and S1 genes inserted into NDV genome under control of transcriptional gene end (GE) and gene start (GS) signals. The names, position, and direction of the primers used are shown with arrows (blacks) indicating the size products. (**C**) The insertion of the expression cassette into the non-coding region between the P/M genes of NDV genome was verified by RTPCR using the junction primers NDV-3LS1-2020-F1 and NDV-3LS1-2020-R1, as shown in (B).

Figure 2. Expression of SARS-CoV-2 RBD and S1 proteins in infected Vero E6 cells and NDV particles. (**A)** Western blot detection for the HN-RBD and S1-F proteins expression. Vero E6 cells were infected with the rLS1, rLS1 rLS1-HN-RBD, and rLS1-S1-F viruses at an MOI of 1.0. After 48 hpi, the cells were lysed and analyzed by western blotting. (**B)** To verify the incorporation of the HN-RBD and S1-F proteins into rLS1-HN-RBD, and rLS1-S1-F viruses, the viral particles in allantoic fluid of infected SPF chicken embryonated eggs with the recombinant viruses and rLS1, was concentrated by ultracentrifugation, and partially purified on a 25 % sucrose cushion. Western blot analysis was carried out using partially purified viruses and lysate from infected cells, using a rabbit antibody specific to SARS-CoV-2 RBD protein and Anti Rabbit IgG conjugated to HRP. The black arrow indicates the expected protein band. The gels are shown with equal running conditions. (**C**) Vero-E6 cells infected with the rLS1, rLS1-HN-RBD, and rLS1-S1-F at an MOI of 0.5. After 48 h, the expression of RBD and S1 proteins was detected by Immunofluorescence assay using a rabbit antibody specific to SARS-CoV-2 RBD protein, and a Donkey Anti-Rabbit IgG H&L-Alexa Fluor 594. Therefore, the NDV was detected using a chicken antiserum specific to the NDV, and a Goat Anti-Chicken IgY H&L-Alexa Fluor® 488. Cell nuclei were stained with DAPI. A scale bar of 50-µm. Image magnification 200x. (**D**) Detection of S1 or RBD proteins on the viral surface of rLS1-S1-F and rLS1-HN-RBD viruses' attachment to Vero E6 cells was performed in two independent experiments. The cells were incubated with purified viruses rLS1-HN-RBD or rLS1-S1-F, for 30 min. Subsequently, the cells were labeled with rabbit monoclonal antibody anti-SARSCOV-2 S1 as the primary antibody, followed by secondary antibody goat anti-rabbit IgG Alexa Fluor 488.
The cells were then analyzed by a flow cytometer. The percentage of positive cells indicates the detection of S1 or RBD proteins on the viral surface of viruses bound to Vero E6 and is shown in the dot plot for rLS1S1-F virus and sLS1 -HN-RBD virus; including negative controls for each assay determined by cells incubated with phosphate-buffered saline (PBS) or rLS1 virus.

Figure 3. The intranasal vaccine elicits specific antibodies against RBD protein and neutralizing antibodies against SARS-CoV-2 in hamsters. (**A**) Immunization regimen. To evaluate the immunogenicity of the NDV vaccines, five-week-old female and male golden Syrian hamsters were used in this study. The hamsters were randomly divided into five groups. The hamsters were vaccinated by intranasal route with live NDV vaccine, following a prime-boost-regimen with a two-week interval. Group 1 received rLS1-HN-RBD (*n*=12), Group 2 received the rLS1-S1-F (n=12), Group 3 received the mixture of rLS1-HN-RBD/rLS1-S1-F (*n*=12), Group 4 did not receive any vaccine (n=12) and served as a positive control group, and Group 5 receive no vaccine and was not challenged, hence serving as a healthy control group (*n*=12). One booster immunization with the same concentration of each vaccine was applied in all vaccinated groups at the second week. (**B**) ELISA assay to measure SARS-CoV-2 RBD-specific serum IgG antibody, and (**C**) S1 subunit-specific serum IgG antibody. Sera from hamsters at pre-boost and 15 days after boost were evaluated. SARS-CoV-2 RBD purified recombinant protein was used for ELISA. The cutoff was set at 0.06. (**D**). Immunized hamsters were bled preboost and 15 days after boost. All sera were isolated by low-speed centrifugation. Serum samples were processed to evaluate the neutralizing antibody titers against SARS-CoV-2 RBD protein using the surrogate virus neutralization test (sVNT). The positive cut-off and negative cut-off for SARS-CoV-2 neutralizing antibody detection were interpreted as the inhibition rate. The cut-off interpretation of results: result positive ≥20% (neutralizing antibody detected), result negative <20% (neutralizing antibody no detectable). (**E**) Figure depicts titers of plaque reduction neutralization test (PRNT) of SARS-CoV-2 on Vero cells with pooled serum from hamsters immunized with rLS1-S1-F, rLS1-HN-RBD, and the mixture of both. (**F**) Plaque reduction (%) curves using pooled serum from the different groups of hamsters. Two-way ANOVA and Tukey's post hoc were performed. *: P < 0.05. **: P < 0.01. ***: P < 0.001. ****: p < 0.0001.

Figure 4. Cellular immunity. These figures show cytokines measured by quantitative ELISA (pg/ml) on hamster serum immunized with rLS1-HN-RBD (n=3), rLS1-S1-F (n=3 for IFNγ, n=2 for IL-2), rLS1-HNRBD/rLS1-S1-F (n=3) and mock (n=2) at 15 DPV. (**A**) IL-2 and (**B**) IFNγ. ns: not significant; P <0.05. Fold expression of cytokines by ΔΔqPCR from hamster spleens (n=13) vaccinated with rLS1-HN-RBD (n=4), rLS1-S1-F (n=4), rLS1-HN-RBD/rLS1-S1-F (n=4), and mock (n=1). IFNγ (**C**), TNFα (**D**), and IL-10 (**E**), were evaluated at 15 DPV. Each individual present 3 technical replicas for GOI and 2 technical replicas for HKG, a No-RT control was included. Non-parametric Mann-Whitney-Wilcoxon test was used with Stata software v.16. P values of <0.05 were considered significant. * P <0.05, ** P <0.01, *** P <0.001, **** P<0.0001. NS, not significant

Figure 5. Efficacy of live NDV vaccines against SARS-CoV-2 infection in hamsters. Golden Syrian hamsters groups vaccinated with rLS1-S1-F, rLS1-HN-RBD, the mixture rLS1-S1-F/rLS1-HN-RBD, and negative control (not immunized) were challenged 30 days after the boost with SARS-CoV-2; an unimmunized and unchallenged group was also included (Mock). (**A**) Viral isolation (%) was done from the lung of each hamster group (n=4) at days 2, 5, and 10 post-challenge. Two-way ANOVA and Tukey's post hoc were performed. *: P < 0.05. **: P < 0.01. ***: P < 0.001. ****: P < 0.0001. (**B**) Detection by qRT-PCR of SARSCoV-2 in culture supernatant of Vero cells, inoculated with immunized and challenged hamster lung homogenates. The data show a significant difference in the Ct value * P <0.05, ** P <0.01, *** P <0.001, **** P <0.0001. NS, not significant. (**C**) Lung histopathology

of each hamster group (n=4) was euthanized at different days post-infection (DPI). Hemorrhagic and infiltrated areas are indicated by a yellow and black arrow, respectively. Image amplitude: 20x. Scale-bar: 100 µm.

Figure 6. Body weight and mobility analysis of SARS-CoV-2 challenged golden Syrian hamsters. (**A**) Changes in body weight (percent weight change compared to day 0) of hamsters inoculated with SARS-CoV2 and Mock group, at days 2, 5, and 10 post-challenged. Mobility assessment results shown (**B**) average velocity, (**C**) average acceleration, and (**D**) average displacement. Mean ± s.d. are shown. Asterisks indicate that results were statistically significant compared to the control group ($P<0.05$).

FUNDING

This study was funded by FARVET. The National Council of Science and Technology from Peru (CONCYTEC-FONDECYT) supported FARVET in the construction of the BSL3 facility where the challenge study in hamsters was performed.

ACKNOWLEDGEMENTS

We thank the National Institute of Health from Peru (INS) for providing the SARS-CoV-2 virus aliquots and for their participation in the virus neutralization, viral load and viability tests. We are grateful for the excellent technical assistance, fruitful discussions and selfless support to the development of the project done by Dr. Paquita Garcia, Dr. Henri Bailon, MSc. Miryam Palomino, Lic. Maribel Huaringa, and BSc. Pamela Ríos researchers of the Laboratory of Virology of the INS.

We acknowledge Dr. Maria Salas, for her advice in the toxicity study. We are grateful to Dr. Daniela Kirwan, Dr. Valerie Paz-Soldan, Dr. Gabriela Salmon, and doctoral candidate David Requena for their comments and criticisms to the manuscript.

PATENT

Peruvian patent # N33-2021/DIN has been filed for the vaccine candidates presented in this study.

COMPETING INTERESTS

The authors declare no competing interests.

REFERENCES

1. Gallagher, T. M. & Buchmeier, M. J. Coronavirus spike proteins in viral entry and pathogenesis. *Virology* **279**, 371–374 (2001).

2. Gorbalenya, A. E. *et al.* The species Severe acute respiratory syndrome-related coronavirus: classifying 2019-nCoV and naming it SARS-CoV-2. *Nat. Microbiol.* **5**, 536–544 (2020).

3. Walls, A. C. *et al.* Structure, function, and antigenicity of the SARS-CoV-2 spike glycoprotein. *Cell* **181**, 281-292.e6 (2020).

4. Huang, J. *et al.* Priming with SARS CoV S DNA and boosting with SARS CoV S epitopes specific for CD4+ and CD8+ T cells promote cellular immune responses. *Vaccine* **25**, 6981– 6991 (2007).

5. Yu, M. *et al.* Determination and application of immunodominant regions of SARS coronavirus spike and nucleocapsid proteins recognized by sera from different animal species. *J. Immunol. Methods* **331**, 1–12 (2008).

6. Du, L. *et al.* The spike protein of SARS-CoV - A target for vaccine and therapeutic development. *Nat. Rev. Microbiol.* **7**, 226–236 (2009).

7. Ma, C. *et al.* Searching for an ideal vaccine candidate among different MERS coronavirus receptor-binding fragments-the importance of immunofocusing in subunit vaccine design. *Vaccine* **32**, 6170–6176 (2014).

8. Ahmed, S. F., Quadeer, A. A. & McKay, M. R. Preliminary identification of potential vaccine targets for the COVID-19 coronavirus (SARS-CoV-2) based on SARS-CoV immunological studies. *Viruses* **12**, (2020).

9. Requena, D., Médico, A., Chacón, R. D., Ramírez, M. & Marín-Sánchez, O. Identification of novel candidate epitopes on SARS-CoV-2 proteins for South America: A review of HLA frequencies by country. *Front. Immunol.* **11**, 1–16 (2020).

10. Dai, L. & Gao, G. F. Viral targets for vaccines against COVID-19. *Nat. Rev. Immunol.* **21**, 73–82 (2021).

11. Guruprasad, L. Human SARS CoV-2 spike protein mutations. *Proteins Struct. Funct. Bioinforma.* 1–8 (2021) doi:10.1002/prot.26042.

12. Zhang, L. *et al.* SARS-CoV-2 spike-protein D614G mutation increases virion spike density and infectivity. *Nat. Commun.* **11**, 1–9 (2020).

13. Greaney, A. J. *et al.* Complete mapping of mutations to the SARS-CoV-2 spike receptorbinding domain that escape antibody recognition. *Cell Host Microbe* **29**, 44-57.e9 (2021).

14. Van Egeren, D. *et al.* Risk of evolutionary escape from neutralizing antibodies targeting SARS-CoV-2 spike protein. *medRxiv* (2020) doi:10.1101/2020.11.17.20233726.

15. Ou, X. *et al.* Characterization of spike glycoprotein of SARS-CoV-2 on virus entry and its immune cross-reactivity with SARS-CoV. *Nat. Commun.* **11**, (2020).

16. Garcia-Beltran, W. F. *et al*. Multiple SARS-CoV-2 variants escape neutralization by vaccine-induced humoral immunity. *Cell,* (2021) doi:10.1016/j.cell.2021.03.013.

17. Zhou, D. et al. "Evidence of escape of SARS-CoV-2 variant B.1.351 from natural and vaccine-induced sera." Cell, S0092-8674(21)00226-9. 23 Feb. 2021, doi:10.1016/j.cell.2021.02.037.

18. World Health Organization. Covid-19 Situation report. *World Health Organ.* **31**, 61–66 (2020).

19. Buschmann, M. D. *et al.* Nanomaterial delivery systems for mRNA vaccines. *Vaccines* **9**, 1– 30 (2021).

20. Dong, Y. *et al.* A systematic review of SARS-CoV-2 vaccine candidates. *Signal Transduct. Target. Ther.* **5**, (2020).

21. Amanat, F. & Krammer, F. SARS-CoV-2 Vaccines: Status report. *Immunity* **52**, 583–589 (2020).

22. Bashir Bello, M. *et al.* Exploring the prospects of engineered Newcastle disease virus in modern vaccinology. *Viruses* **12**, 1–23 (2020).

23. Kim, S. H. & Samal, S. K. Newcastle disease virus as a vaccine vector for development of human and veterinary vaccines. *Viruses* **8**, (2016).

24. Abozeid, H. H. *et al.* Development of a recombinant Newcastle disease virus-vectored vaccine for infectious bronchitis virus variant strains circulating in Egypt. *Vet. Res.* **50**, 1–13 (2019).

25. ICTV. International committee on taxonomy of viruses. https://talk.ictvonline.org/taxonomy/ (2019).

26. Diel, D. G. *et al.* Complete genome and clinicopathological characterization of a virulent Newcastle disease virus isolate from South America. *J. Clin. Microbiol.* **50**, 378–387 (2012).

27. Miller, P. J. & Koch, G. *Newcastle disease. In: Swayne, D.E., Glisson, J.R., McDougald, L.R., Nolan, L.K., Suarez, D.L., Nair, V. Diseases of Poultry* (2013). doi:10.1016/B978-012-804607-4.00020-4.

28. Bukreyev A., Collins P.L. Newcastle disease virus as a vaccine vector for humans. *Curr Opin Mol Ther.* 10, 46–55 (2008).

29. Freeman, A. I. *et al.* Phase I/II trial of intravenous NDV-HUJ oncolytic virus in recurrent glioblastoma multiforme. *Mol. Ther.* **13**, 221–228 (2006).

30. Schirrmacher, V. Cancer vaccines and oncolytic viruses exert profoundly lower side effects in cancer patients than other systemic therapies: A comparative analysis. *Biomedicines* **8**, (2020).

31. Burman, B., Pesci, G. & Zamarin, D. Newcastle disease virus at the forefront of cancer immunotherapy. *Cancers (Basel).* **12**, 1–15 (2020).

32. Duan, Z., Xu, H., Ji, X. & Zhao, J. Recombinant Newcastle disease virus-vectored vaccines against human and animal infectious diseases. *Future Microbiol.* **10**, 1307–1323 (2015).

33. Shirvani, E., Paldurai, A., Manoharan, V. K., Varghese, B. P. & Samal, S. K. A recombinant Newcastle disease virus (NDV) expressing S protein of infectious bronchitis virus (IBV) protects chickens against IBV and NDV. *Sci. Rep.* **8**, 1–14 (2018).

34. Saikia, D. P. *et al.* Recombinant Newcastle disease virus (NDV) expressing Sigma C protein of avian reovirus (ARV) protects against both ARV and NDV in chickens. *Pathogens* **8**, 145 (2019).

35. DiNapoli, J. M. *et al.* Newcastle disease virus, a host range-restricted virus, as a vaccine vector for intranasal immunization against emerging pathogens. *Proc. Natl. Acad. Sci. U. S. A.* **104**, 9788–9793 (2007).

36. Liu, R. Q. *et al.* Newcastle disease virus-based MERS-CoV candidate vaccine elicits highlevel and lasting neutralizing antibodies in Bactrian camels. *J. Integr. Agric.* **16**, 2264–2273 (2017).

37. Sun, W. *et al.* A Newcastle disease virus (NDV) expressing a membrane-anchored spike as a cost-effective inactivated SARS-CoV-2 vaccine. *Vaccines* **8**, 1–14 (2020).

38. Sun, W. *et al.* Newcastle disease virus (NDV) expressing the spike protein of SARS-CoV-2 as a live virus vaccine candidate. *EBioMedicine* **62**, (2020).

39. Xiaojie, S., Yu, L., lei, Y., Guang, Y. & Min, Q. Neutralizing antibodies targeting SARSCoV-2 spike protein. *Stem Cell Res.* **50**, (2021).

40. Gavor, E., Choong, Y. K., Er, S. Y., Sivaraman, H. & Sivaraman, J. Structural basis of SARS-CoV-2 and SARS-CoV antibody interactions. *Trends Immunol.* **41**, 1006–1022 (2020).

41. Zhang, H. *et al.* Identification of an antigenic determinant on the S2 domain of the severe acute respiratory syndrome coronavirus spike glycoprotein capable of inducing neutralizing antibodies. *J. Virol.* **78**, 6938–6945 (2004).

42. Imai, M. *et al.* Syrian hamsters as a small animal model for SARS-CoV-2 infection and countermeasure development. *Proc. Natl. Acad. Sci. U. S. A.* **117**, 16587–16595 (2020).

43. Sia, S. F. *et al.* Pathogenesis and transmission of SARS-CoV-2 in golden hamsters. *Nature* **583**, 834–838 (2020).

44. Park, J.-G. *et al.* Immunogenicity and protective efficacy of an intranasal live-attenuated vaccine against SARS-CoV-2 in preclinical animal models. *bioRxiv* 2021.01.08.425974 (2021).

45. Bukreyev, A. *et al.* Recombinant Newcastle disease virus expressing a foreign viral antigen is attenuated and highly immunogenic in primates. *J. Virol.* **79**, 13275–13284 (2005).

46. Nelson, C. B., Pomeroy, B. S., Schrall, K., Park, W. E. & Linderman, R. J. An outbreak of conjunctivitis due to Newcastle disease virus (NDV) occurring in poultry workers. *Am. J. Public Health Nations. Health* **42**, 672–678 (1952).

47. Lam, H. Y. *et al.* Corrigendum to 'safety and clinical usage of Newcastle disease virus in cancer therapy'. *Biomed Res. Int.* **2017**, 4529437 (2017).

48. Izquierdo-Lara, R., Chumbe, A., Calderón, K., Fernández-Díaz, M. & Vakharia, V. N. Genotype-matched Newcastle disease virus vaccine confers improved protection against genotype XII challenge: The importance of cytoplasmic tails in viral replication and vaccine design. *PLoS One* **14**, 1–16 (2019).

49. Zhao, W. *et al.* Newcastle disease virus (NDV) recombinants expressing infectious laryngotracheitis virus (ILTV) glycoproteins gB and gD protect chickens against ILTV and NDV challenges. *J. Virol.* **88**, 8397–8406 (2014).

50. Mebrahtu, K., Teshale, S., Esatu, W., Habte, T. & Gelaye, E. Evaluation of spray and oral delivery of Newcastle disease I2 vaccine in chicken reared by smallholder farmers in central Ethiopia. *BMC Vet. Res.* **14**, 1–7 (2018).

51. Ma, J. *et al.* Newcastle disease virus-based H5 influenza vaccine protects chickens from lethal challenge with a highly pathogenic H5N2 avian influenza virus. *npj Vaccines* **2**, 1–10 (2017).

52. Dimitrov, K. M., Afonso, C. L., Yu, Q. & Miller, P. J. Newcastle disease vaccines—a solved problem or a continuous challenge? *Vet. Microbiol.* **206**, 126–136 (2017).

53. Cardenas-Garcia, S. *et al.* Molecular epidemiology of Newcastle disease in Mexico and the potential spillover of viruses from poultry into wild bird species. *Appl. Environ. Microbiol.* **79**, 4985–4992 (2013).

54. Cornax, I., Miller, P. J. & Afonso, C. L. Characterization of live LaSota vaccine straininduced protection in chickens upon early challenge with a virulent Newcastle disease virus of heterologous genotype. *Avian Dis.* **56**, 464–470 (2012).

55. Boumart, Z. *et al.* Thermal stability study of five Newcastle disease attenuated vaccine strains. *Avian Dis.* **60**, 779–783 (2016).

56. Torjesen, I. Covid-19 will become endemic but with decreased potency over time, scientists believe. *BMJ* 18–19 (2021) doi:10.1136/bmj.n494.

57. Alexandra B Hogan *et al.* Report 33 - Modelling the allocation and impact of a COVID-19 vaccine. *Imp. Coll. London Rep.* (2020).

58. Chumbe, A., Izquierdo-Lara, R., Calderón, K., Fernández-Díaz, M. & Vakharia, V. N. Development of a novel Newcastle disease virus (NDV) neutralization test based on recombinant NDV expressing enhanced green fluorescent protein. *Virol. J.* **14**, 1–11 (2017).

59. Peeters, B. P. H., Gruijthuijsen, Y. K., De Leeuw, O. S. & Gielkens, A. L. J. Genome replication of Newcastle disease virus: Involvement of the rule-of-six. *Arch. Virol.* **145**, 1829–1845 (2000).

60. World Organization for Animal Health. *OIE Manual of diagnostic tests and vaccines for terrestrial animals (mammals, birds and bees). OIE Manual of Diagnostic Test and Vaccines for Terrestrial Animals Seventh Edition, 2012* vol. 2 (2012).

61. Mendoza, E. J., Manguiat, K., Wood, H. & Drebot, M. Two Detailed Plaque Assay Protocols for the Quantification of Infectious SARS-CoV-2. *Curr. Protoc. Microbiol.* **57**, 1– 15 (2020).

62. Timiryasova, T. M. *et al.* Optimization and validation of a plaque reduction neutralization test for the detection of neutralizing antibodies to four serotypes of dengue virus used in support of dengue vaccine development. *Am. J. Trop. Med. Hyg.* **88**, 962–970 (2013).

63. Boudewijns, R. *et al.* STAT2 signaling restricts viral dissemination but drives severe pneumonia in SARS-CoV-2 infected hamsters. *Nat. Commun.* **11**, 1–10 (2020).

64. Chan, J. F., Zhang, A. J., Yuan, S. & Kwok-Y, Y. Simulation of the clinical and pathological manifestations of Coronavirus Disease 2019 (COVID-19) in golden Syrian hamster model: implications for disease pathogenesis and transmissibility. *Clin Infect Dis.* **2019**, 1–50 (2019).

65. Ribeiro-Romão, R. P., Saavedra, A. F., Da-Cruz, A. M., Pinto, E. F. & Moreira, O. C. Development of real-time PCR assays for evaluation of immune response and parasite load in golden hamster (Mesocricetus auratus) infected by Leishmania (Viannia) braziliensis. *Parasites and Vectors* **9**, 1–12 (2016).

66. Espitia, C. M. *et al.* Duplex real-time reverse transcriptase PCR to determine cytokine mRNA expression in a hamster model of New World cutaneous leishmaniasis. *BMC Immunol.* **11**, (2010).

67. Livak, K. J. & Schmittgen, T. D. Analysis of relative gene expression data using real-time quantitative PCR and the 2-ΔΔCT method. *Methods* **25**, 402–408 (2001).

68. Padilla-Rojas C, Lope-Pari P, Vega- Chozo K, Balbuena-Torres J, Caceres-Rey O, BailonCalderon H, Huaringa-Nuñez M, R.-S. N. 2020. Near-complete genome sequence of a 2019 novel coronavirus (SARS-CoV-2) strain causing a COVID-19 case in Peru. *Microbiol Resour Announc 9e00303-20* **9**, 1–3 (2020).

69. João F. Henriques, Caseiro Rui, Martins Pedro & Batista Horge. High-speed tracking with kernelized correlation filters. *IEEE Trans. Pattern Anal. Mach. Intell.* **37**, 583–596 (2015).

CONSORTIUM

Members of the COVID-19 Working Group in Perú:

Katherine Calderon[1, 4], Aldo Rojas-Neyra[1, 4], Angela Montalvan[1], Dora Rios-Matos[1], Astrid Poma-Acevedo[1], Ricardo Choque-Guevara[1], Kathy Pauyac[1], Norma Perez-Martinez[1], Manuel CriolloOrozco[1], Elmer Delgado-Ccancce[1], Yacory Sernaque-Aguilar[1], Doris Villanueva-Pérez[1], Freddy Ygnacio-Aguirre[1], Ricardo Montesinos-Millan[1], Naer Chipana-Flores[1], Edison HuaccachiGonzalez[1], Pedro Huerta-Roque[1], Gisela Isasi-Rivas[1], Kristel Gutiérrez[1], Andres Agurto-Arteaga[1], Abraham Licla-Inca[1], Yudith Cauna-Orocollo[1], Maria de Grecia Cauti-Mendoza[1], Ricardo Antiparra[1], Manuel Ardiles-Reyes[1], Xiomara Chunga-Girón[1], Lewis De La Cruz[1], Nicolás E. Delgado-Pease[1], Christian Elugo-Guevara[1], Oscar Heredia-Almeyda[1], Gabriel Jiménez-Avalos[1], Romina A. Juscamaita-Bartra[1], Dennis Núñez-Fernández[1], Adiana Ochoa-Ortiz[1], Gustavo E. Olivos-Ramirez[1], Erika Páucar-Montoro[1], Jose L. Perez-Martinez[1], Stefany Quiñones-Garcia[1], Ingrid Ramirez-Ortiz[1], Daniel Ramos-Sono[1], Angela A. Rios-Angulo[1], Yomara K. Romero[1], Mario I. Salguedo-Bohorquez[1], Luis F. Soto[1], Luis Tataje-Lavanda[1], Katherine Vallejos-Sánchez[1], A. Paula Vargas-Ruiz[1], Renzo G. Villena[1], Patricia Sheen[1], Julio Ticona[1], Manolo FernándezSanchez[1], Vikram N. Vakharia[2], Eliana Icochea[1,3], Luis Guevara-Sarmiento[1], Mirko Zimic[1], Manolo Fernández-Díaz[1]

AFILITIONS

[1]Farmacológicos Veterinarios S.A.C. FARVET
[2]Institute of Marine and Environmental Technology, University of Maryland Baltimore County, Baltimore, USA

[3]Laboratorio de Patología Aviar. Facultad de Medicina Veterinaria. Universidad Nacional Mayor de San Marcos, Lima, Perú
[4]Universidad Nacional San Luis Gonzaga, Ica, Perú

AUTHOR CONTRIBUTION STATEMENT

MFD, MZ, and LGS, conceived the study and experiments. KC and ARN produced the NdV vaccine. MFD, MZ, LGS, KC, ARN, APA, KVS, YCO, SQG and CWGP developed the protocols. KC, ARN, APA, AM, IR, DRM, AAA, MGCM, GIR, KGM, NPM, YSA, FYA, DVP, RCG, RMM, IRO, JT, MFS and GIR carried out the experiments. MSB, DNF, LTL, CWGP and MZ planned and carried out the simulations. DNF and MSB analyzed the videos for mobility evaluation. MCO, EHG, EDC and KPA

contributed to sample preparation. MZ, MFD, KC, ARN, VV, APA, DRM, EI and LGS analyzed and interpreted the results. MFD, MZ, LGS, KC, ARN, VV, SQG, ARA, KVS and YCO took the lead in writing the manuscript. MFD funded the study. All authors provided critical feedback and helped shape the research, analysis and manuscript.

ADDITIONAL INFORMATION

Supplementary material accompanies this paper.

DATA AVAILABILITY

All relevant data are contained within the manuscript and the supplementary material. Additional raw data will be available upon request.

FIGURES

Figure 1

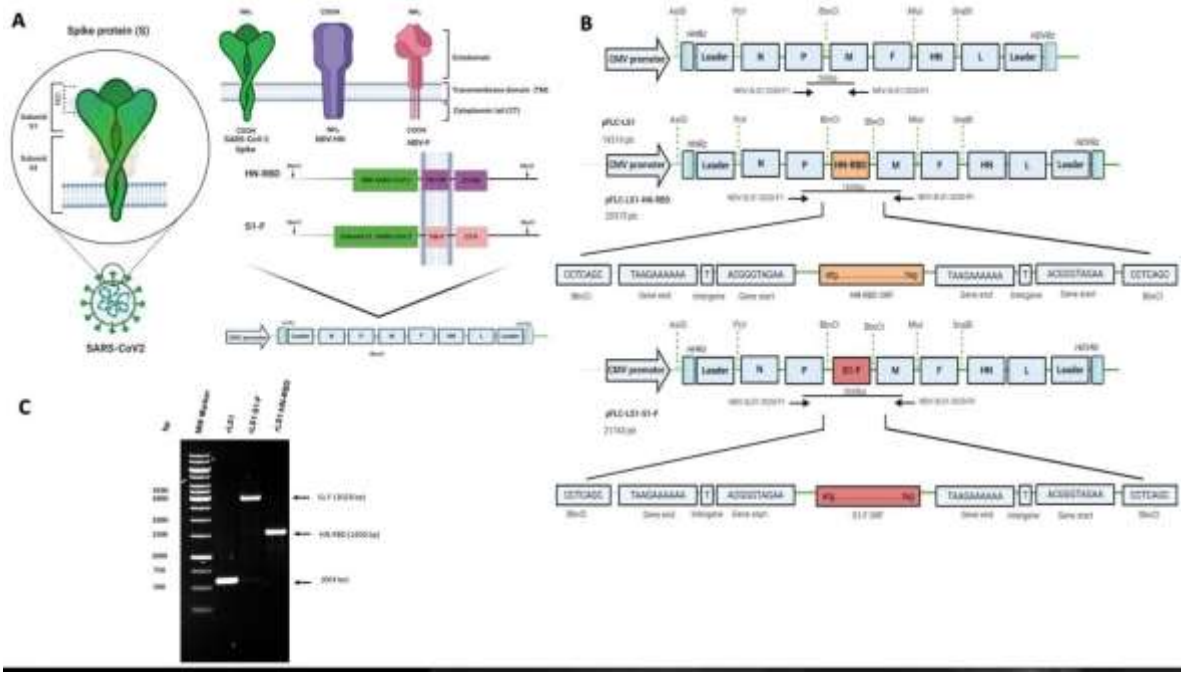
A
Spike protein (S)
SARS-CoV2
HN-RBD
S1-F
B
CMV promoter
Leader
N
P
M
F
HN
L
C
MW Marker

986 Figure 2

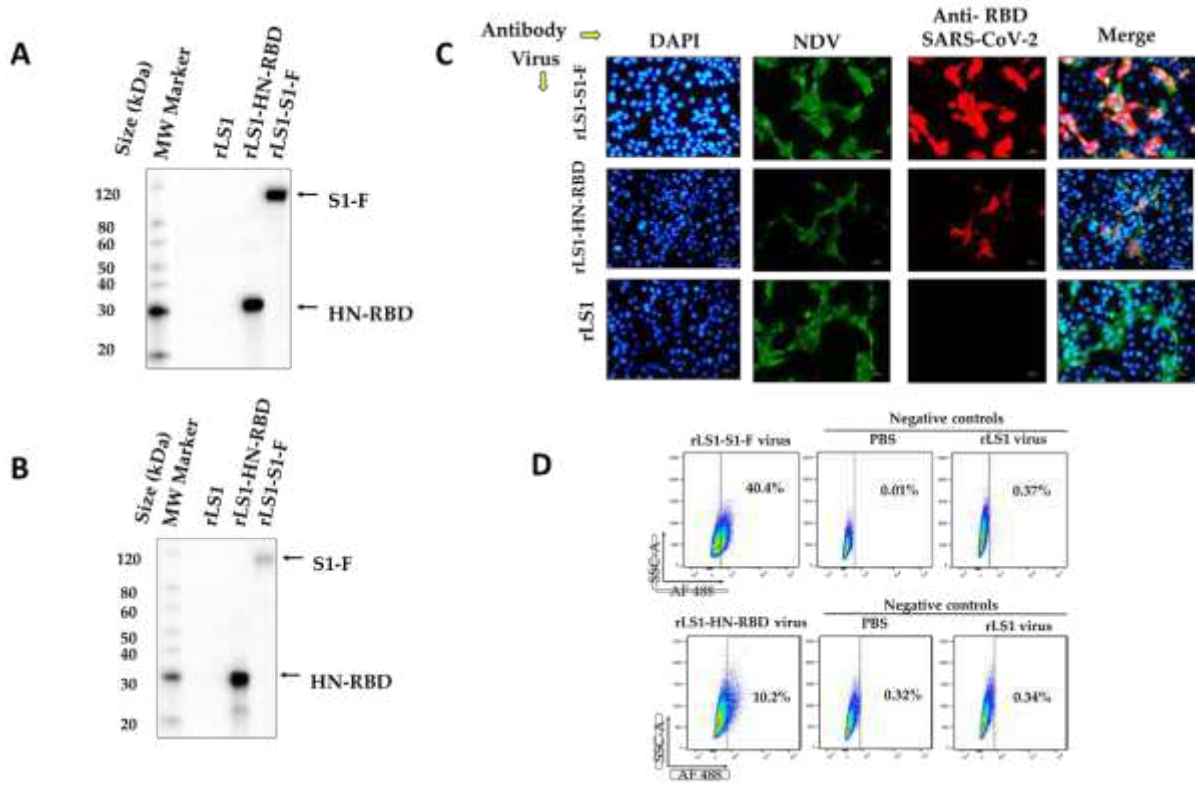

987

988 Figure 3

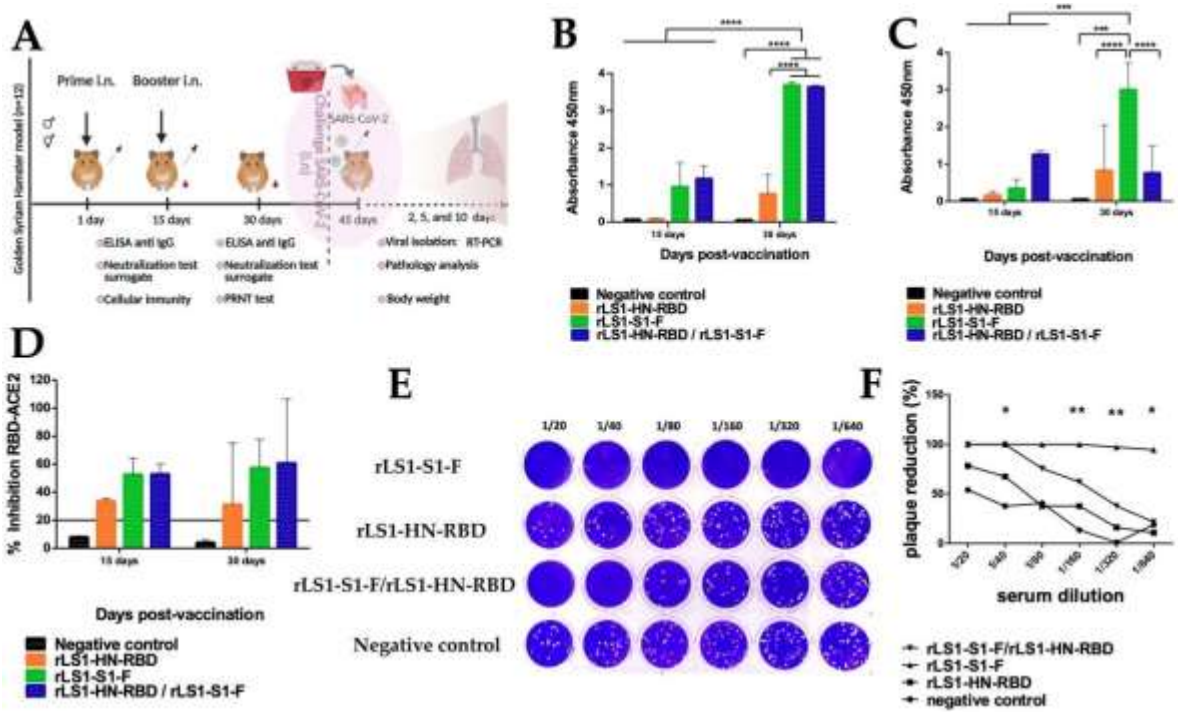

989
990
991
992
993
994
995
996
997
998
999
1000
1001

Figure 4

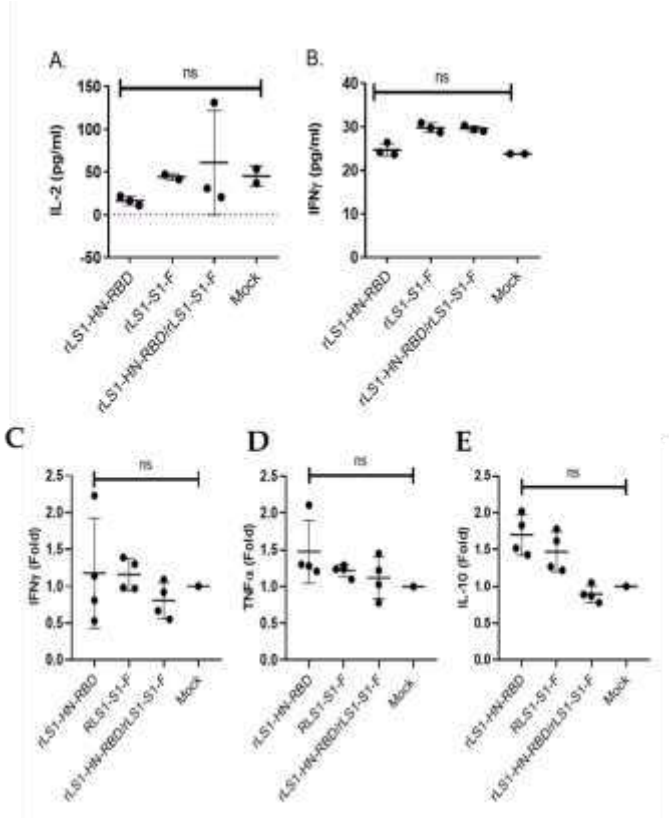
A.
ns
IL-2 (pg/ml)
150
100
50
0
-50
rLS1-HN-RBD
rLS1-S1-F
rLS1-HN-RBD/rLS1-S1-F
Mock
B.
ns
IFNγ (pg/ml)
40
30
20
10
0
rLS1-HN-RBD
rLS1-S1-F
rLS1-HN-RBD/rLS1-S1-F
Mock
C
ns
IFNγ (Fold)
2.5
2.0
1.5
1.0
0.5
0.0
rLS1-HN-RBD
RLS1-S1-F
rLS1-HN-RBD/rLS1-S1-F
Mock
D
ns
TNFα (Fold)
2.5
2.0
1.5
1.0
0.5
0.0
rLS1-HN-RBD
RLS1-S1-F
rLS1-HN-RBD/rLS1-S1-F
Mock
E
ns
IL-10 (Fold)
2.5
2.0
1.5
1.0
0.5
0.0
rLS1-HN-RBD
RLS1-S1-F
rLS1-HN-RBD/rLS1-S1-F
Mock

1027 1096 Figure 5

1028

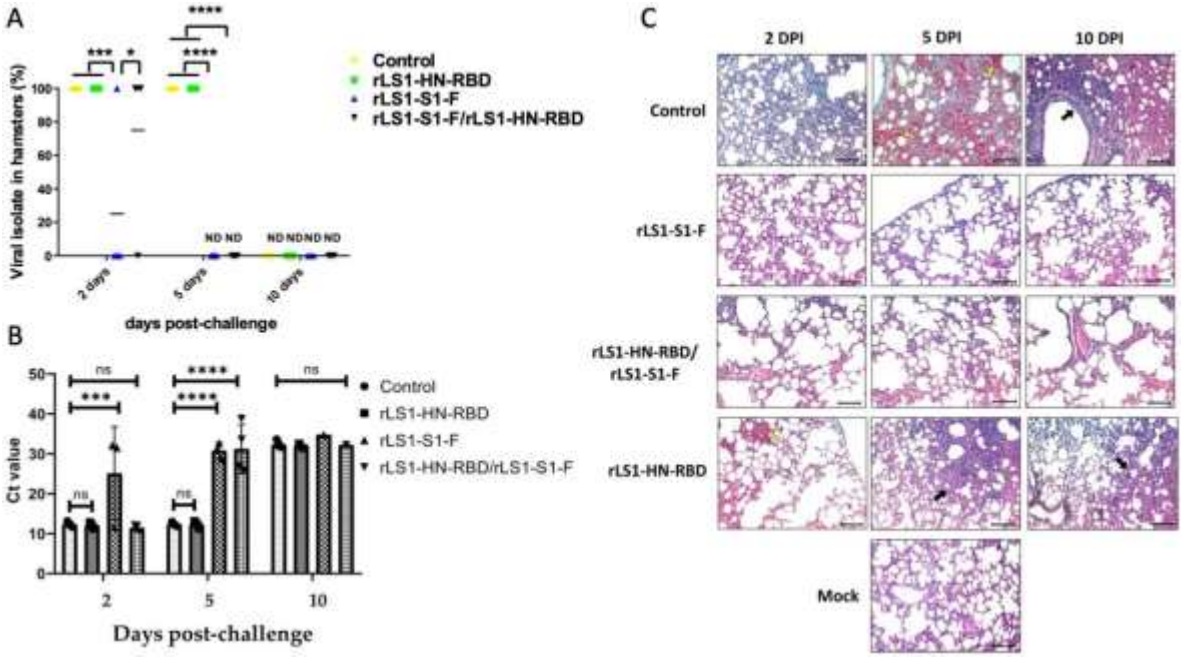

1029

1030

1031

1032

1033

1034

1035

1036

1037

1038

1039

1040

1041

Figure 6

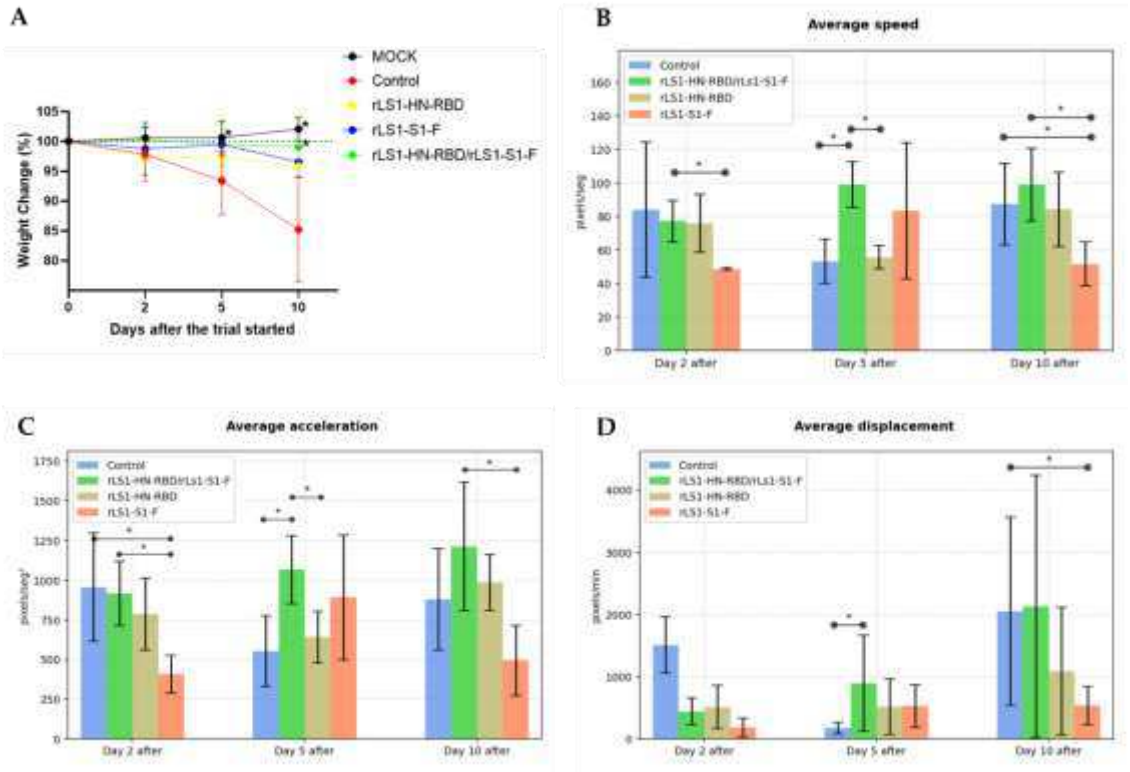
A
MOCK
Control
rLS1-HN-RBD
rLS1-S1-F
rLS1-HN-RBD/rLS1-S1-F
Weight Change (%)
Days after the trial started
B
Average speed
C
Average acceleration
D
Average displacement
Day 2 after
Day 5 after
Day 10 after

1053
1054
1055
1056
1057
1058
1059
1060
1061
1062
1063

Figures

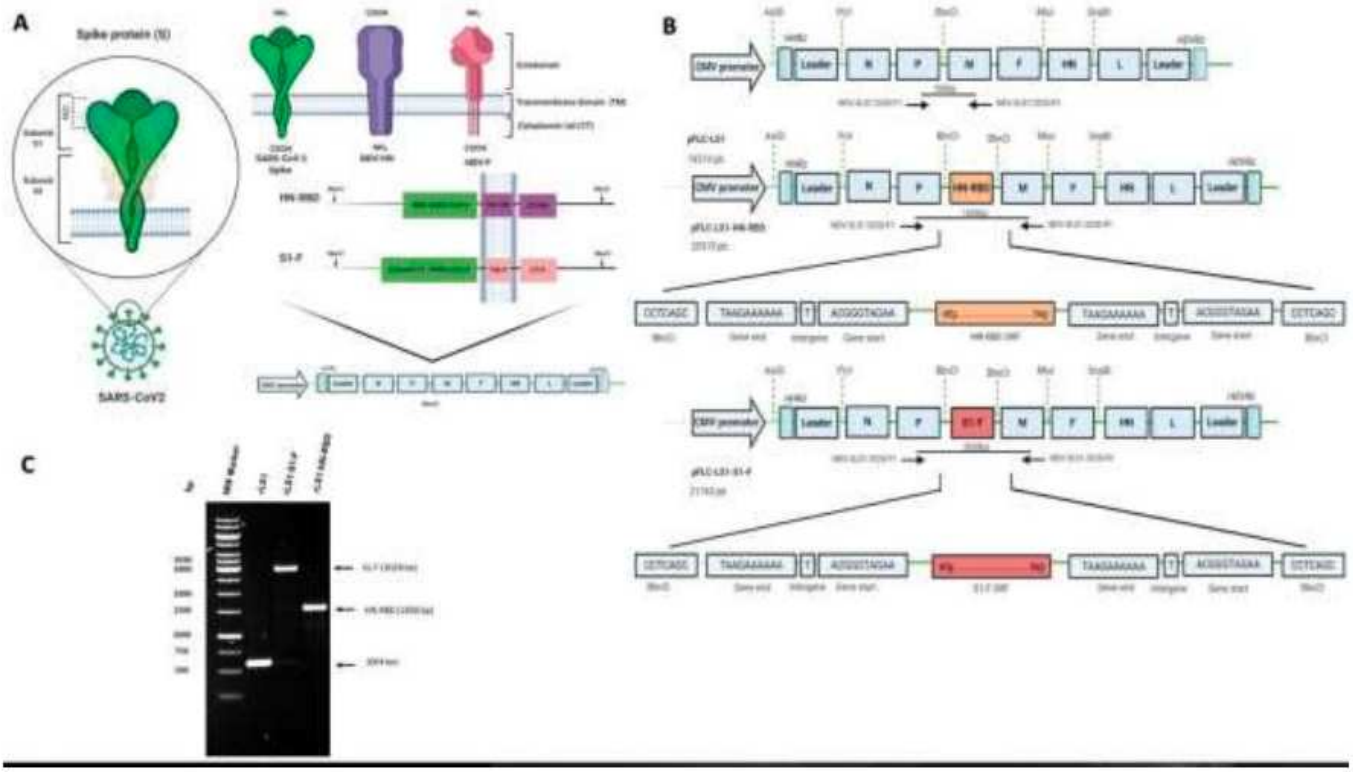

Figure 1

Please see the Manuscript PDF file for the complete figure caption

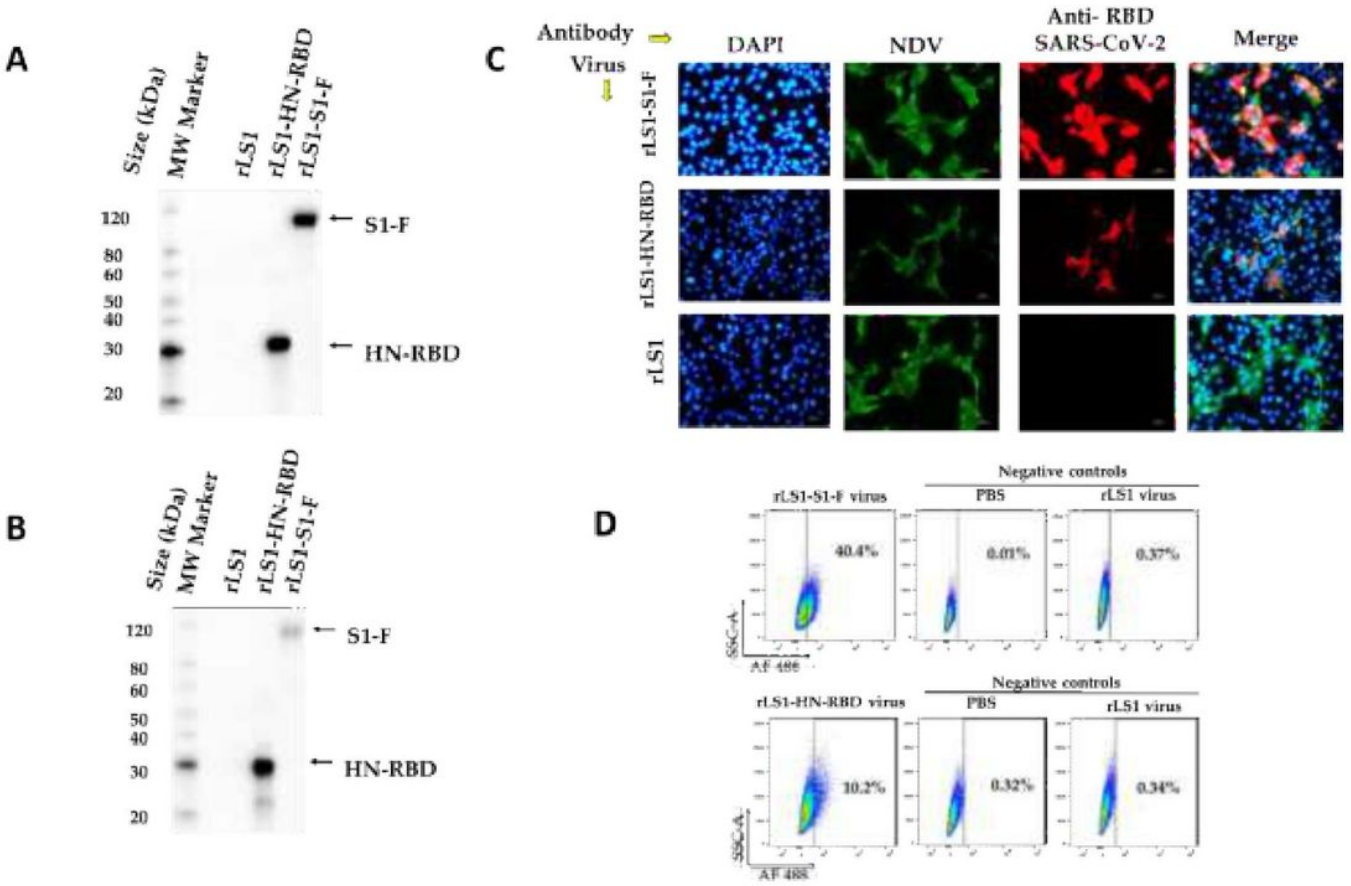

Figure 2

Please see the Manuscript PDF file for the complete figure caption

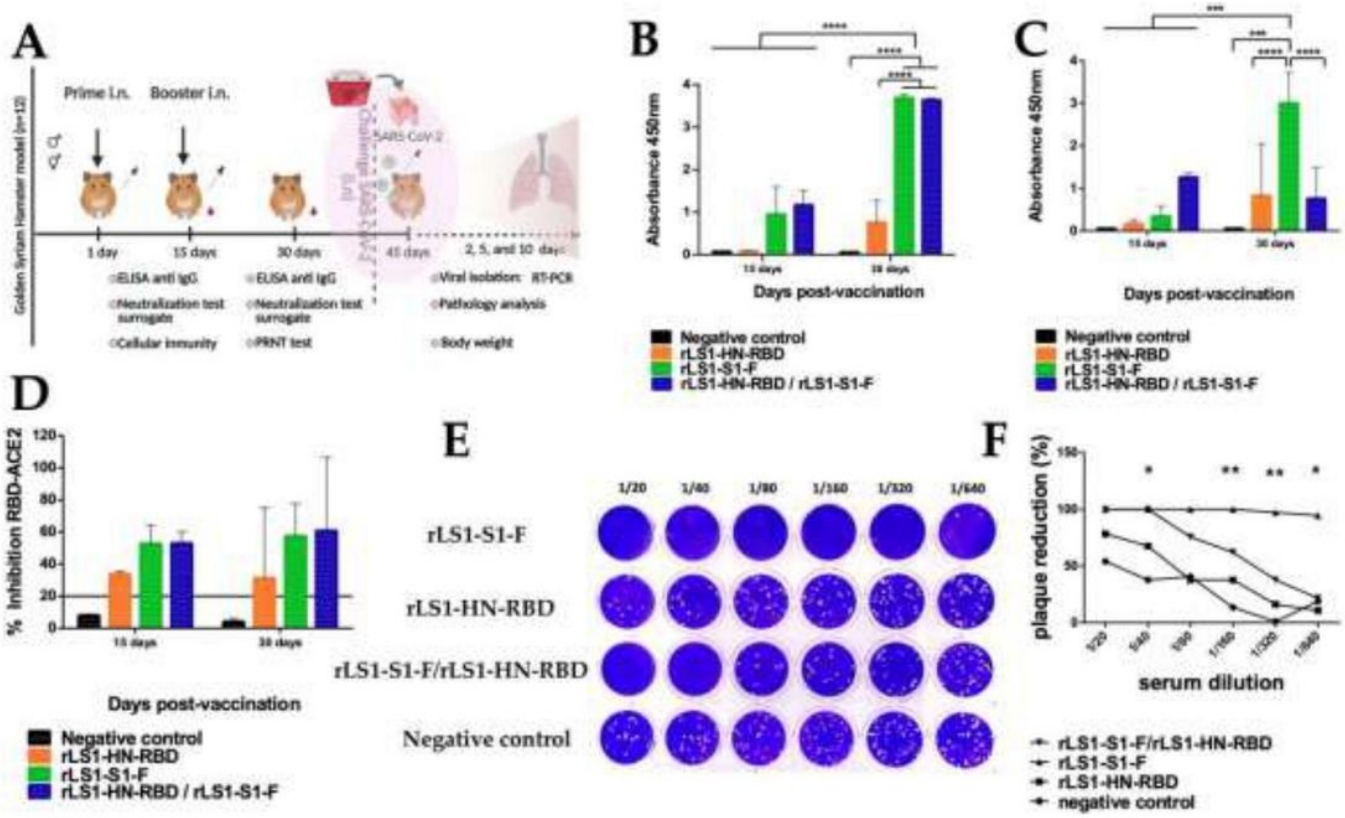

Figure 3

Please see the Manuscript PDF file for the complete figure caption

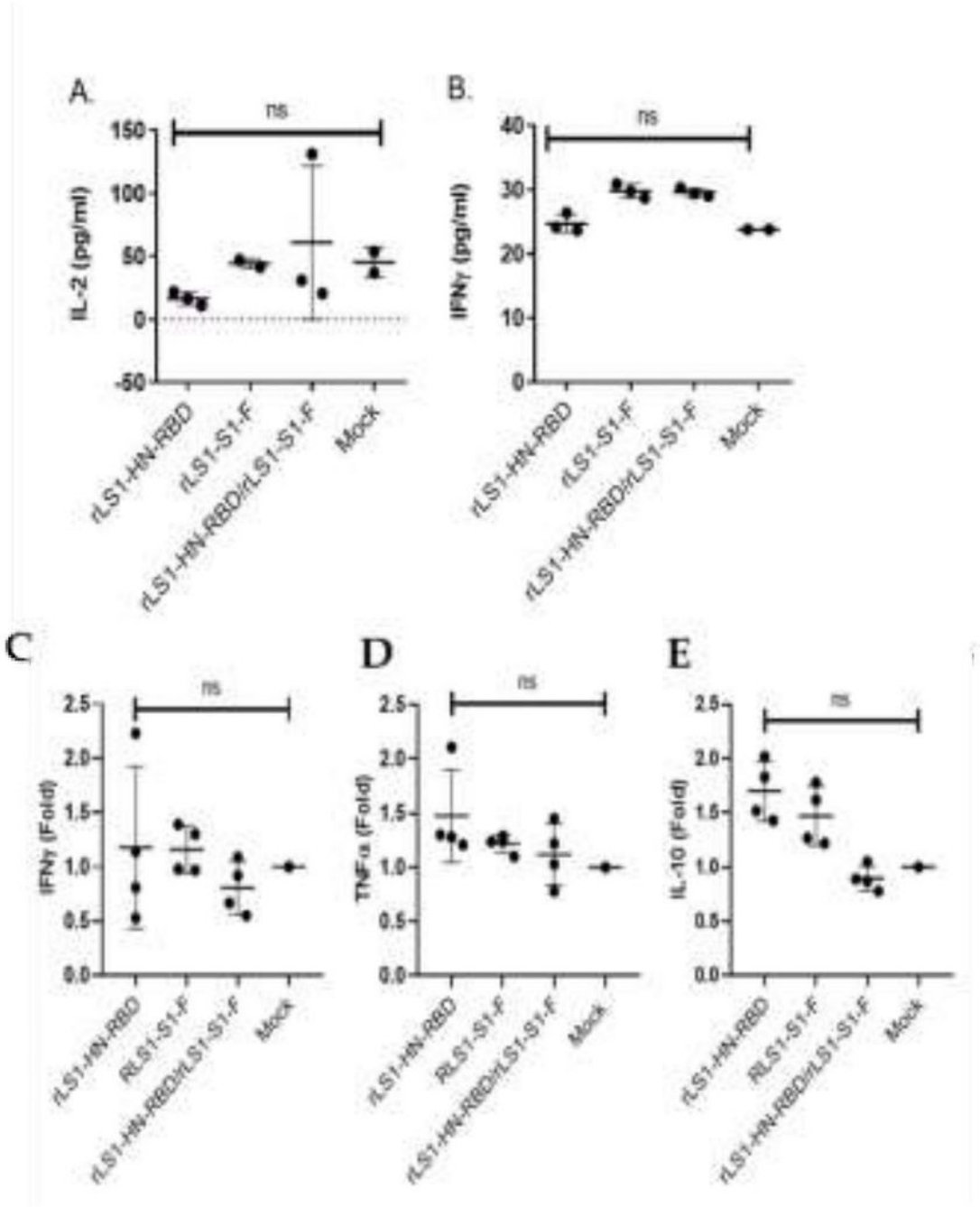

Figure 4

Please see the Manuscript PDF file for the complete figure caption

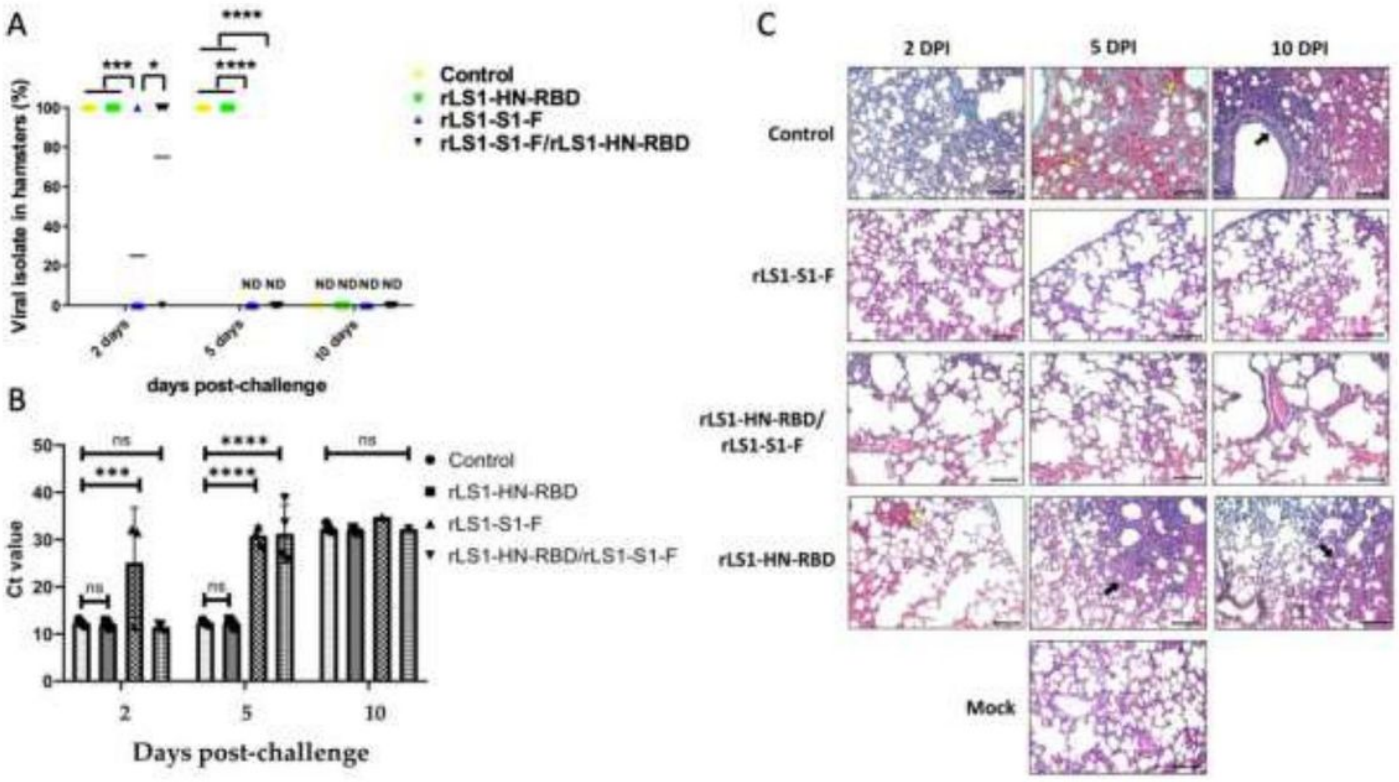

Figure 5

Please see the Manuscript PDF file for the complete figure caption

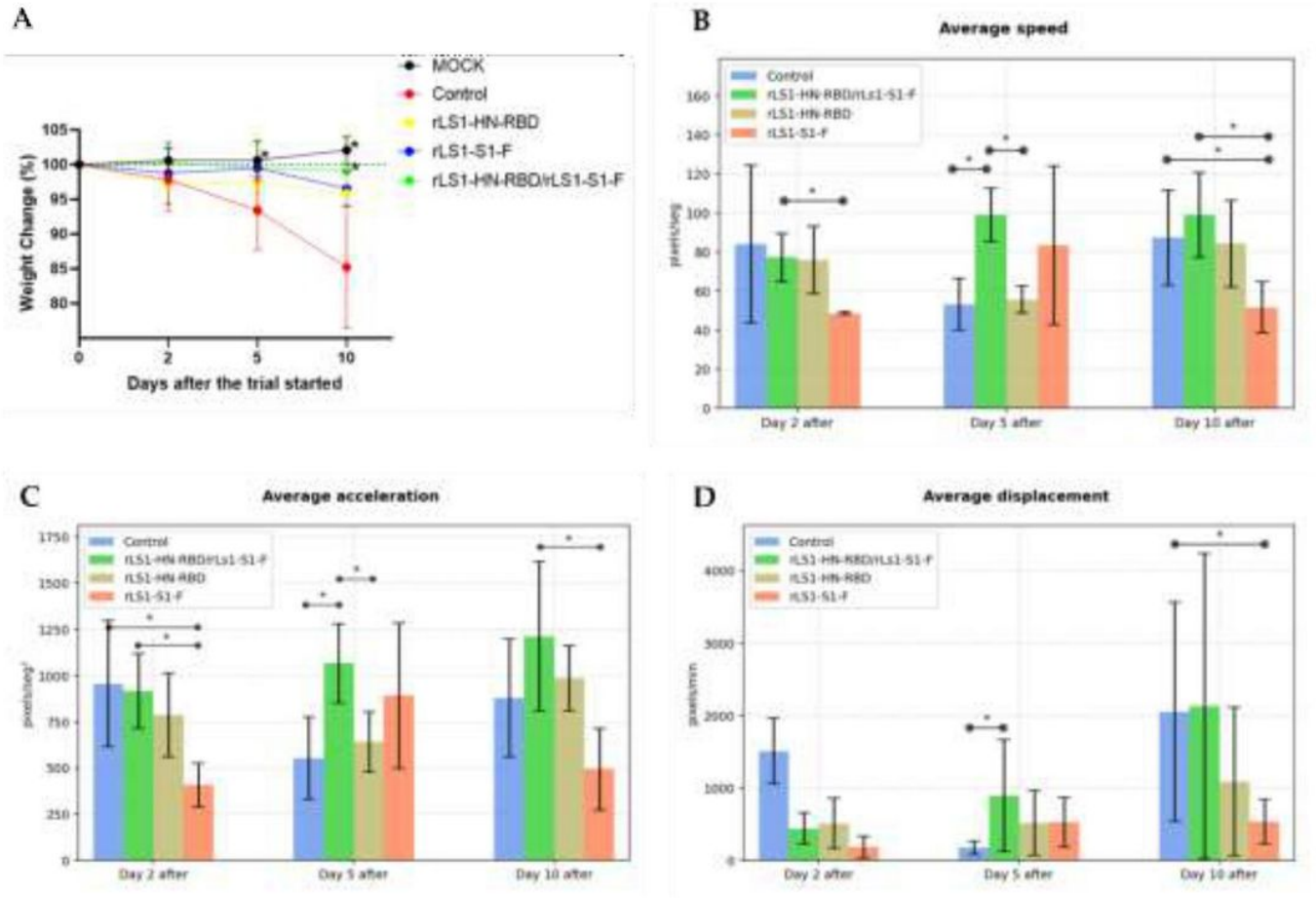

Figure 6

Please see the Manuscript PDF file for the complete figure caption

Supplementary Files

This is a list of supplementary files associated with this preprint. Click to download.

- SUPPLEMENTARYMATERIAL.pdf